Electron–nuclear double resonance of impurity centers in nonmetallic crystals

B. G. Grachev and M. F. Deĭgen

Institute of Semiconductors, Academy of Sciences of the Ukrainian SSR, Kiev
Usp. Fiz. Nauk **125**, 631–663 (August 1978)

This review presents briefly the ideas underlying the electron–nuclear double resonance (ENDOR) method and also discusses methods for the analysis of spectra with the aim of obtaining information on the hyperfine and quadrupole interactions of paramagnetic centers with lattice nuclei and illustrates the potentialities of the ENDOR method in the determination of the structure and properties of impurity centers. Apart from these traditional topics, the attention is concentrated on new aspects of the ENDOR method: influence of external agencies (electric field, pressure, and temperature) on the ENDOR spectra, ENDOR dynamics, optical detection, etc. A demonstration is given of the capabilities of the ENDOR method in investigations of the fundamental characteristics of crystals, such as the energy band structure, local properties near defects, spin–phonon interaction characteristics, excited states of local centers, etc. This demonstration is illustrated by examples of ENDOR studies of electron and hole centers in insulators and semiconductors.

PACS numbers: 76.70.Dx, 61.70.Rj

CONTENTS

1. INTRODUCTION

In 1944, E. K. Zavoĭskiĭ discovered resonant absorption of microwave radiation as a result of transitions between electron spin energy levels, now known as electron spin resonance (ESR), and thus founded rf spectroscopy. Only a few years later it became clear that rf spectroscopy is not only of scientific but also of practical importance. The evidence for this was provided by A.M. Prokhorov, N.G. Basov, and C.H. Townes, who founded quantum electronics. In 1956, Feher[1] suggested that transitions between nuclear spin sublevels - nuclear magnetic resonance (NMR) - could be detected on the basis of their influence on the ESR signal. This generalization of the ESR method, usually called electron–nuclear double resonance (ENDOR), has proved to be exceptionally fruitful. The ENDOR method combines the high sensitivity of the ESR with the high resolution of the NMR and makes it possible to obtain valuable information on paramagnetic centers in insulator and semiconductor crystals, ferroelectrics, organic crystals, liquids, and powders.

Good introductions to the ENDOR method are provided by some of the published reviews.[2-7] Seidel and Wolf[2] collected the results of the first measurements of the hyperfine and quadrupole interaction constants of color centers in alkali halide crystals. Later[3] they analyzed comprehensively the rf spectroscopy of color centers in alkali halides; part of their review is devoted to the ENDOR of the F, F_A, V_K, and some other centers. The ENDOR method is analyzed in other reviews.[4,7] Chapter IV in the momograph of Abragam and Bleaney[5] gives an excellent introduction to ENDOR of transition ions. A concise review of most of the ENDOR work done up to 1970 can be found in Kwiram's review.[6]

Our task will not be to discuss all the ENDOR investigations (since the appearance of Kwiram's review,[6] which has a bibliography of 300 items, the number of publications on this method has at least doubled).

The purpose of the present review is to demonstrate the capabilities of the ENDOR method. The ENDOR spectra are known to give important information on the nature of paramagnetic centers and on the distribution of electron clouds in these centers. However, these capabilities are manifested particularly strikingly in studies of the influence of external agencies on the spectra, in analysis of the ENDOR dynamics, and in methods of optical detection of the ENDOR signal. These methods make it possible to determine not only the properties of paramagnetic centers but also the fundamental characteristics of the host crystal itself. These new aspects will be the main concern of the present review.

By way of illustration, we shall consider electron and

 0038-5670/78/080674-19$01.10

hole centers in alkali halides, donors in silicon, and some other impurity centers in nonmetallic crystals.

2. UNDERLYING IDEAS AND DATA-GATHERING POTENTIALITIES OF THE ENDOR METHOD

The processes which occur in real objects and which give rise to an ENDOR signal are very complex and not yet fully understood. However, in some limiting cases they can be interpreted clearly and described mathematically in quite a simple manner.

a) We shall consider two cases frequently encountered in experiments:

A) at low temperatures in the case of adiabatically fast passage through resonance we can ignore the relaxation phenomena in a system of electron and nuclear spins;

B) the relaxation processes are completed in a time much shorter than the observation time.

For simplicity, we shall confine our attention to paramagnetic centers with electron spin 1/2 and one nucleus of spin 1. The splitting of the energy levels of such a paramagnetic center subjected to a static external magnetic field H is determined by the Zeeman interaction of the electron S and nuclear I spins with a magnetic field, hyperfine interaction between an electron and a nucleus, and nuclear quadrupole interaction (Fig. 1a). We shall use M and m for the projections of the electron and nuclear spins along the quantization axis. Transitions with $\Delta M=0$, $\Delta m\neq 0$ are nuclear and those with $\Delta M\neq 0$, $\Delta m=0$ are ESR transitions.

A. Figure 1a shows the level populations under thermal equilibrium conditions. The application of a high-power microwave signal at the frequency of one of the ESR transitions (Fig. 1b) equalizes the populations of the levels involved and microwave power is no longer absorbed (saturation state). Now an rf signal is applied and its frequency is varied. When the rf quantum energy $h\nu_{EN}$ coincides with one of the differences between the nuclear sublevel energies (for example $|\frac{1}{2}1\rangle$ and $|\frac{1}{2}0\rangle$), nuclear transitions are induced and the level populations are redistributed (Fig. 1c). Since this alters the difference between the populations of the $|\frac{1}{2}0\rangle$ and $|-\frac{1}{2}0\rangle$ levels, absorption appears at the ESR frequency ν_e. The change in the ESR signal due to the excitation of transitions between nuclear sublevels is known as ENDOR and the frequencies ν_{EN} at which this occurs are the ENDOR frequencies.

B. Possible relaxation transitions between the levels of a paramagnetic center are shown in Fig. 2a. Let us assume that an external microwave field induces transitions with $\Delta M=\pm 1$, $\Delta m=0$, $m=1$ (see Fig. 2b) and let the probability of these transitions be P_e. In this case the intensity of the ESR signal is governed by the competition between different relaxation processes. There are at least two relaxation channels between the levels $|\frac{1}{2}1\rangle$ and $|-\frac{1}{2}1\rangle$: the direct relaxation process with a characteristic time τ_1 and an indirect process via an intermediate level $|\frac{1}{2}0\rangle$. The latter is a sequence of two relaxation stages with times τ_n and τ_x and it is usually much slower if τ_1, $\tau_x\ll\tau_n$. An rf signal at a frequency ν_{EN} induces nuclear transitions whose probability is P_n and if $P_n\gg\tau_x^{-1}$, the indirect relaxation time decreases considerably (it becomes equal to τ_x instead of τ_n even in the absence of rf radiation). The resultant change in the ESR signal, i.e., the ENDOR signal, can then be recorded. Variation of the intensity of the rf (nuclear) radiation and of the amplitude of the microwave field makes it possible to select the optimal observation conditions.

In both cases A and B the measured quantities are the ENDOR frequencies ν_{EN}. They are governed by the splittings of the paramagnetic center levels (Fig. 1), which can be described conveniently by the spin Hamiltonian

$$\mathcal{H}=\beta \mathbf{S}g\mathbf{H}-\beta_n\mathbf{I}g_n\mathbf{H}+\mathbf{S}A\mathbf{I}+\mathbf{I}Q\mathbf{I} \qquad (2.1)$$

where β, β_n and g, g_n are the electron and nuclear magnetons and spectroscopic splitting tensors, respectively; A and Q are the hyperfine and quadrupole interaction tensors.

The ENDOR method allows us to find the components

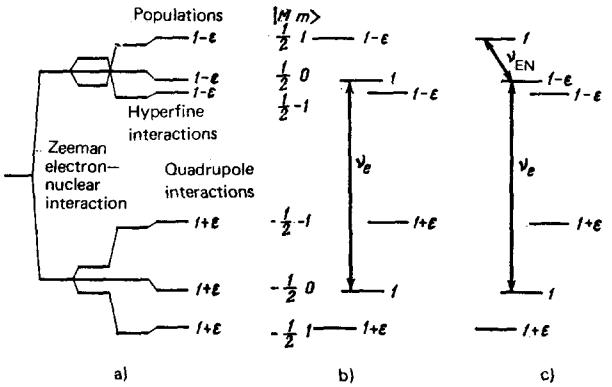

FIG. 1. Transient ENDOR. The energy scheme shows levels of a paramagnetic center with $S=\frac{1}{2}$, $I=1$ in a static external magnetic field. The relative populations are given alongside each level as follows: a) under thermal equilibrium conditions ($\varepsilon=g\beta H/2k_BT$, $\varepsilon\ll 1$); b) in the presence of a saturating microwave field; c) after the action of an rf field at one of the ENDOR frequencies ν_n.

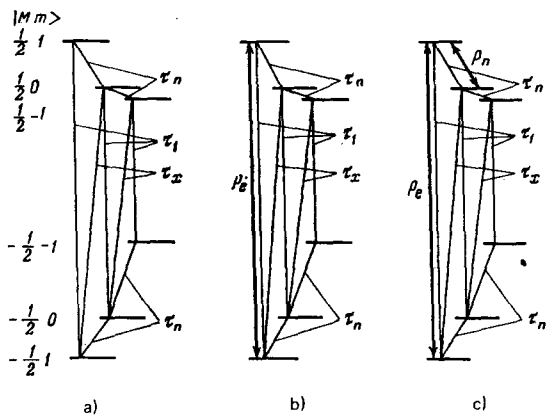

FIG. 2. Steady-state ENDOR: a) relaxation processes in the $S=\frac{1}{2}$, $I=1$ system with an isotropic hyperfine interaction; b) in the presence of an external microwave field; c) in the presence of an rf field.

of g_n, A, and Q and their relative signs. If a paramagnetic-center electron interacts with several nuclei, the components of the tensors can be found for each of them.

The advantages of the ENDOR method is the high precision of the determination of the hyperfine and quadrupole interaction constants. This is achieved because the lines are narrow compared with the ESR case. Typical ESR lines are inhomogeneously broadened by local fields, such as those created by the lattice nuclei surrounding a paramagnetic center. The same fields broaden also the ENDOR lines but their influence on the nuclear transitions is β_n/β times less than on electron transitions. It is worth noting that the sensitivity of the ENDOR method is also several times higher than that of the NMR method, mainly becuase a microwave quantum whose absorption is facilitated by an rf quantum is much greater than the latter. Larger quanta are easier to detect. This sensitivity makes it possible to investigate nuclear spin transitions by the ENDOR method, whose number is too small for NMR observations, and this can be done in particular for nuclei near paramagnetic centers.

We shall now consider why the quantities which can be determined by the ENDOR method are of interest.

The theory of electrostatic and magnetic interactions of electrons and nuclei (see, for example, Refs. 5 and 8) shows that in the case of an unpaired electron,

$$a^{(i)} = \frac{1}{3}\,\mathrm{Sp}\,A^{(i)} = \frac{8\pi}{3} g\beta g_n \beta_n |\psi(\mathbf{R}^{(i)})|^2; \qquad (2.2)$$

here, $\mathbf{R}^{(i)}$ is the position vector of the i-th nucleus: ψ is the electron wave function; $a^{(i)}$ is known as the isotropic or contact hyperfine interaction constant.

If g and g_n are known, we can use Eq. (2.2) to find the square of the modulus of the electron wave function at the point of location of a nucleus from the measured isotropic hyperfine interaction constant. If the constants of the hyperfine interaction of an electron with several n - clei in its vicinity are known from the ENDOR experiments it is possible to determine the distribution of the localized electron density in a crystal. In this sense the ENDOR apparatus acts as a "$|\psi|^2$ meter."

The quadrupole interaction constants are proportional to the electric-field gradient created by the charges of paramagnetic centers at a nucleus and can be used to determine the relative positions of charges in the lattice. The anisotropic part of the hyperfine interaction gives information on the relative positions of the lattice nuclei with which a paramagnetic-center electron interacts.

For the majority of nuclei the spectroscopic splitting factor is a scalar quantity equal to μ_I/I, where μ_I is the magnetic moment of the nucleus in nuclear magnetons. However, in the case of paramagnetic ions with closely spaced excited electron states the nuclear factor g_n becomes anisotropic and may differ from μ_I/I. This can be detected by the ENDOR method.

The constants $g_n^{(i)}$, $a^{(i)}$, $A_{pq}^{(i)}$, and $Q_{pq}^{(i)}$ do not exhaust the list of quantities which can be determined by the ENDOR method. The same method can be used to find the changes in the hyperfine and quadrupole interaction

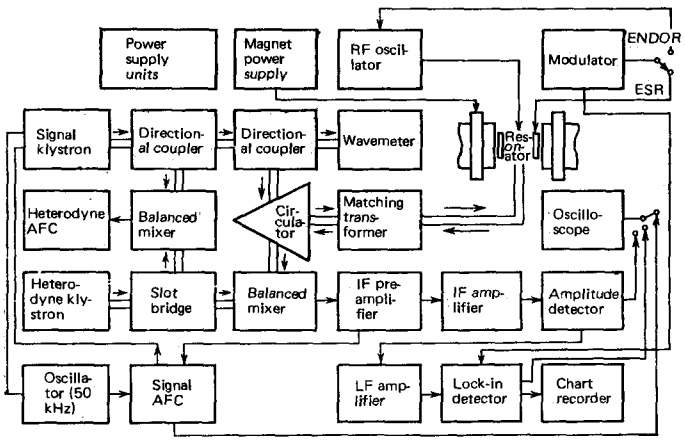

FIG. 3. Functional circuit of an ÉYa-1301 ENDOR spectrometer.

constants on application of external agencies (electric field, pressure, temperature) to a crystal. Investigations of the ENDOR line intensities and dynamics make it possible to study the processes of nuclear and electron spin–lattice relaxation and to determine the relevant relaxation times.

b) Experimental technique. Since the ENDOR signal represents only a few percent of the ESR signal, a highly sensitive spectrometer is needed.[9] Until recently, superheterodyne spectrometers have been usually employed and they operate most effectively under microwave saturation conditions. A gradual transition is now taking place to simpler and more convenient modulation spectrometers, because improved models of these instruments can operate without a significant loss of sensitivity at low modulation frequencies. Figure 3 and 4 give the functional circuit diagram and show the external appearance of an ENDOR spectrometer developed at the Institute of Semiconductors of the Ukrainian Academy of Sciences in Kiev in cooperation with the Special Design Bureau of Analytic Instrument Construction in Leningrad.[10] A detailed description of the ENDOR technique can be found, for example, in original papers.[11-14]

c) The varied information which is provided by the ENDOR experiments can be utilized provided we carry out the following two tasks: i) describe the frequencies and intensities of ENDOR transitions by a set of constants of a phenomenological spin Hamiltonian; ii) calculate microtheoretically these constants so as to express

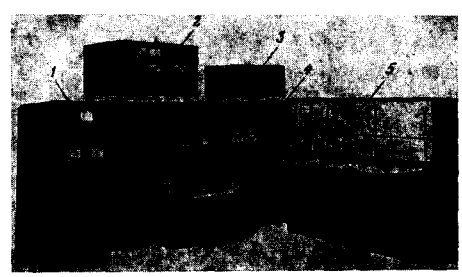

FIG. 4. External appearance of an ÉYa-1301 ENDOR spectrometer: 1) electromagnetic power supply; 2) microwave unit; 3) *rf* unit; 4) electromagnet; 5) recording system.

them in terms of the characteristics of the paramagnetic centers of the crystal which contains them. The general principles for tackling the first task are now known and for most of the cases encountered in practice it has been done quite fully. In the next two sections we shall consider the method for the determination of the constants of the hyperfine and quadrupole interaction of a localized electron with the surrounding nuclei on the basis of the ENDOR spectra. We shall also describe some progress in the second task, which is much harder and further from completion (Secs. 8 and 11).

3. THEORY OF ENDOR SPECTRA

The ENDOR spectra of paramagnetic centers in crystals are usually described using a phenomenological spin Hamiltonian. In general, the precision of the ENDOR measurements in such that frequencies have to be found by numerical diagonalization of the spin Hamiltonian on a computer. Such calculations are necessary for the description of fine details of the spectrum.[15] However, qualitative and frequently quantitative analysis of the spectra can be carried out using perturbation theory. This is done by presenting the total spin Hamiltonian in the form

$$\mathcal{H} = \mathcal{H}_{\text{ESR}} + \mathcal{H}_{\text{ENDOR}}. \tag{3.1}$$

The term $\mathcal{H}_{\text{ESR}}$ represents the interactions of a paramagnetic-center electron with an external magnetic field and with the crystal field, as well as the strong hyperfine interactions with the nuclei in a paramagnetic center or with a small number of nuclei in the immediate vicinity of a center. The term $\mathcal{H}_{\text{ENDOR}}$ represents all the nuclear interactions (Zeeman, quadrupole, etc.) and weak hyperfine interactions of a paramagnetic-center electron with nuclei. In magnetic fields usually employed (of the order of 3000 Oe), the term $\mathcal{H}_{\text{ENDOR}}$ can be regarded as a perturbation of $\mathcal{H}_{\text{ESR}}$.

Let us assume that the Schrödinger equation

$$\mathcal{H}_{\text{ESR}} \mid M \rangle = \mathcal{E}_M \mid M \rangle \tag{3.2}$$

has been solved and the nondegenerate values of ε_M as well as the eigenfunctions $|M\rangle$ are known. Then, the frequencies of nuclear transitions can be found using an effective nuclear spin Hamiltonian:[8]

$$\mathcal{H}_{\text{eff}}^{M} = \langle M \mid \mathcal{H}_{\text{ENDOR}} \mid M \rangle + \sum_{M'} \frac{\langle M \mid \mathcal{H}_{\text{ENDOR}} \mid M' \rangle \langle M' \mid \mathcal{H}_{\text{ENDOR}} \mid M \rangle}{\mathcal{E}_M - \mathcal{E}_{M'}} + \ldots. \tag{3.3}$$

The first term in Eq. (3.3) is diagonalized by introducing some nuclear spin quantization axis, whose direction generally does not coincide with the direction of H and depends on M. The principal effects obtained using an expression of the next order of smallness [the second term in Eq. (3.3), describing what are known as second-order effects] involve renormalization of the quadrupole interaction and of the effective magnetic field acting on the nuclear spins, giving rise to the "indirect interaction" of the nuclei via the electron spin [of the type $I_p^{(k)} I_q^{(n)}$]. General expressions for the ENDOR frequencies obtained allowing for all the interactions in Eqs. (3.1) and (3.3) are very cumbersome. It is usual to employ formulas derived for specific experimental situations.[12,13,15-21] In describing phenomena due to the second-order effects, it is usual to retain in Eq. (3.3) only a few interacting nuclei.[16,17,19] Since the indirect interactions are, as demonstrated by Eq. (3.3), of the order of $A_{pq}^2/4g\beta H$, they can be ignored. Moreover, the direct interactions of the nuclei are also negligible. Therefore, Eq. (3.3) reduces to a sum of easily diagonizable one-particle spin Hamiltonians and ENDOR frequencies can be obtained independently for each of the nuclei.

We shall use $\tilde{B}_{pp}^{(i)}$ to denote the principal values of the tensor $B_{pq}^{(i)} = A_{pq}^{(i)} - a^{(i)}\delta_{pq}$, and employ h_p to denote the direction cosines of **H** in the system of the principal axes of the tensor $B_{pq}^{(i)}$ (for the sake of simplicity, $g_n^{(i)}$ and $Q^{(i)}$ are assumed to be scalars). Then, ignoring second-order effects, we find that the ENDOR frequencies—the differences between the energies of the states (3.3) characterized by a finite matrix element of the operator inducing nuclear transitions in the rf range—are

$$\nu_M^{(i)} = |-\nu_n^{(i)} + M(a^{(i)} + \tilde{B}_{xx}^{(i)} h_x^2 + \tilde{B}_{yy}^{(i)} h_y^2 + \tilde{B}_{zz}^{(i)} h_z^2) + (2m-1)Q^{(i)}|, \tag{3.4}$$

where $\nu_n^{(i)} = g_n^{(i)}\beta_n H$. A comparison of the experimental ENDOR frequencies obtained for various orientations of the magnetic field with the predictions given by expressions of the type of (3.4) makes it possible to find the hyperfine and quadrupole interaction constants.

4. INTERPRETATION OF THE ENDOR SPECTRA

The observed ENDOR spectra are usually due to the interaction of a paramagnetic-center electron with a large number of nuclei of different types and, therefore, these spectra are very complex. Nevertheless, there are certain features which frequently allow us to interpret the spectrum unambiguously, i.e., to assign ENDOR lines to specific nuclear transitions, to find the hyperfine and quadrupole interaction constants characterizing these lines, and finally to identify the nuclei in the environment of a paramagnetic center responsible for these interactions. We shall illustrate our discussion by considering the specific case of the F centers in KBr. The ENDOR spectrum of an F center and its model - an electron captured by an anion vacancy - are shown in Figs. 5 and 6.

a) According to Eq. (3.4),

$$\frac{d\nu_M^{(i)}}{dH} \approx |g_n^{(i)}\beta_n|. \tag{4.1}$$

The magnetic moments and nuclear spins are mostly known. Therefore, having determined $d\nu_M^{(i)}/dH$, we can immediately attribute some of the lines in the spectrum to specific nuclei, for example, the nuclei of the host crystal containing paramagnetic centers (in our case, these are the K and Br nuclei) and thus reduce considerably the number of possible attributions of the other lines.

b) Transitions for any nucleus should give rise to $2S+1$ ENDOR lines of frequencies $\nu_M^{(i)}$ (the sum $M = -\frac{1}{2}$ and difference $M = \frac{1}{2}$ frequencies in the case of an F center with $S = \frac{1}{2}$). If $|A_{pq}^{(i)}| \gg \nu_n^{(i)}$, these frequencies are separated by the familiar distance $2\nu_n^{(i)}$ if the second-order effects are ignored [see Eq. (3.4)]. For $|A_{pq}^{(i)}| \ll \nu_n^{(i)}$,

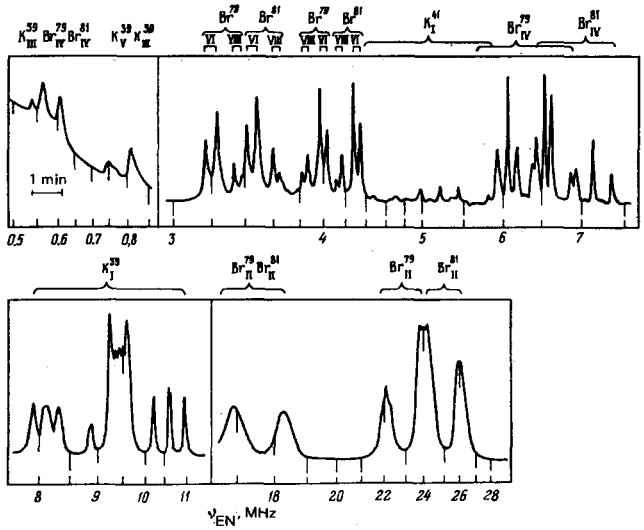

FIG. 5. ENDOR spectra of the F centers in KBr ($H \| \langle 100 \rangle$, $T = 90°K$), taken from Ref. 12.

they are located symmetrically on both sides of $\nu_n^{(i)}$, which helps to identify them (Fig. 5).

c) In interpreting the spectrum one must bear in mind that the quadrupole interaction splits the lines due to individual nuclei to $2I$ components.

d) The second-order effects split additionally the lines of magnetically equivalent nuclei (i.e., nuclei characterized by coincidence of the principal values and directions of the principal axes of the hyperfine and quadrupole interaction tensors).

e) If a crystal contains isotopes, the ENDOR frequencies have characteristic replicas. Since $\nu^{(i)}$ and $A_{pq}^{(i)}$ are proportional to $g_n^{(i)}\beta_n$, it follows that for the nuclei with $Q^{(i)} = 0$ the frequencies of the different isotopes are simply proportional to $g_n^{(i)}\beta_n$. Figure 5 shows clearly the replicas of the ^{79}Br and ^{81}Br lines.

f) The intensity of an ENDOR line is governed by many factors. In particular, it is proportional to the number of nuclei responsible for this line. For example, in the case of isotopes the intensities of the relevant ENDOR lines of crystals which have not been enriched apply to the natural abundances. (The abundances of ^{79}Br and ^{81}Br are almost equal so that the intensities of the lines are the same. The abundance of ^{41}K is 6.8% and, therefore, its line is much weaker than those of ^{39}K.)

g) In the case of a considerable difference between the hyperfine interaction constants in different spheres, the ENDOR lines split into well-defined groups, each of which belongs to a particular sphere ($^{39}K_I$, Br_{II}, and Br_{IV} lines).

h) The anisotropy of the hyperfine and quadrupole interactions makes the ENDOR line positions dependent on the direction of the magnetic field H relative to the principal axes of the hyperfine and quadrupole interaction tensors. Therefore, when the field is rotated, the lines of specific nuclei exhibit characteristic angular dependences. For example, in the case of the six identical nuclei surrounding an F center and located along $\langle 100 \rangle$ axes, the angular dependence is of the kind shown in Fig. 7. In fact, the hyperfine interaction of a paramagnetic-center electron with such nuclei in a cubic crystal has axial symmetry with respect to the vacancy–nucleus axis. Then, according to Eq. (3.4) the ENDOR frequencies depend only on the angle between the symmetry axis and the magnetic field direction. Rotation of the field in a $\{001\}$ plane (see Fig. 7) does not affect the ENDOR frequencies of nuclei 5 and 6 but alters the frequencies of nuclei 1-4 in accordance with a certain law. Such angular dependences are typical of nuclei in the first [001], ninth [003], and other [00k] coordination spheres of an F center.

We shall define a local symmetry group as a set of operations which transform lattice ions into one another but do not affect a paramagnetic center and the investigated nucleus. Then, all the coordination spheres of the nuclei surrounding a substitutional impurity center in a cubic crystal can be divided into classes which differ in respect of the local symmetry group. The angular dependences of the ENDOR lines for spheres of a given class differ qualitatively from one another. Figure 7b shows, by way of illustration, the angular dependence for 12 nuclei of the $\{110\}$ plane class (the second [110] and eighth [220] spheres of an F center). The dependences for spheres of other classes in cubic crystals can be found in the literature.[13,17,22-24]

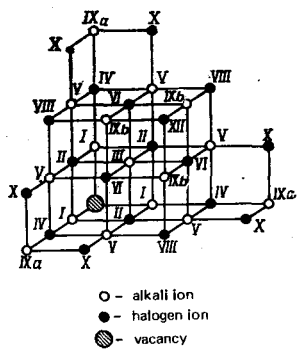

FIG. 6. F center in an alkali halide crystal.

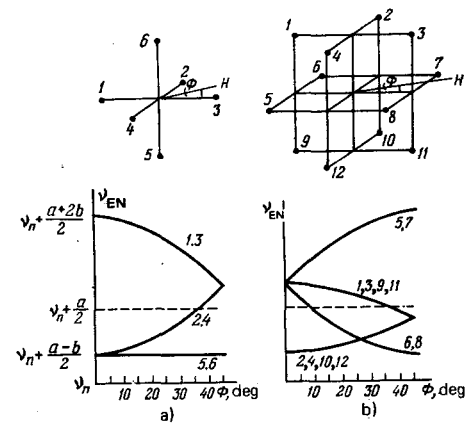

FIG. 7. Angular dependences of the ENDOR sum frequencies of nuclei in $\langle 100 \rangle$ (a) and $\langle 110 \rangle$ (b) classes of spheres in cubic crystals.

Comparing the observed angular dependences with theoretical curves of the type shown in Fig. 7, we can identify all the lines in the spectrum with spheres of nuclei of a specific class of symmetry and select nuclei for each ENDOR line. (For example, this applies to spheres I-VIII of an F center in KBr; the spectrum is shown in Fig. 5.) A numerical comparison of the measured ENDOR frequencies with expressions of the (3.4) type makes it possible to determine the components of the hyperfine and quadrupole interaction tensors.

It should be pointed out that the problem of identifying the nuclei associated with given ENDOR lines is facilitated greatly by theoretical predictions of the values of the hyperfine and quadrupole interaction constants and by further data obtained from ENDOR studies in the presence of external agencies.

i) It follows from Eq. (3.4) that the ENDOR frequencies can be used to find the relative signs of the $g_n^{(i)}$ tensor and of the hyperfine and quadrupole interaction constants. For lack of space, we cannot deal with the methods for the determination of the signs of the constants and would direct the interested reader to the relevant papers.[17,25]

j) A description of the observed angular dependences of the frequencies in the ENDOR spectrum of an F center in an alkali halide crystal is possible only if we adopt the model shown in Fig. 6. Therefore, the ENDOR investigations have made it possible to establish finally the model of an F center in an alkali halide crystal. In the case of paramagnetic centers of unknown structure the ENDOR experiments are capable of giving decisive information on the selection of any specific model.

In the following sections we shall illustrate the potentialities of the ENDOR method in investigations of the structure and various characteristics of a variety of defects using the examples of electron and hole centers in alkali halide and alkaline-earth halide crystals.

5. ENDOR OF ELECTRON COLOR CENTERS

The ENDOR method has found particularly extensive applications in studies of color centers in alkali halide crystals.

a) *F center*. The hyperfine interaction of an F-center electron with nuclei in the first and sometimes second coordination spheres (Fig. 6) has been investigated by the ESR method. The ENDOR method has made it possible to investigate the hyperfine and quadrupole interactions of an F electron with a significantly large number of nuclei in the environment.[2,13,17] The principal values and orientations of the principal axes of the hyperfine and quadrupole interaction tensors have been determined for nuclei in the I-IV coordination spheres for the majority of crystals and in specially favorable cases this has been done also for VIII, IX, and even X spheres.[19,26]

A careful investigation of the ENDOR spectra (in particular, of the nuclei in the first sphere of ^{41}K in KCl and ^{7}Li in LiF - Refs. 16, 17, and 27) has made it possible to detect the theoretically predicted (see Sec. 3) second-order effects, which are the additional splitting

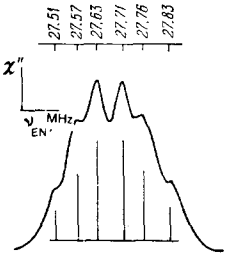

FIG. 8. ENDOR spectrum of a pair of ^{7}Li nuclei in sphere I of an F center in LiF (Ref. 17). $H\|\langle 100\rangle$, $T = 20$ °K. The vertical segments, separated by $2\gamma \approx (a_{Li})^2/2g\beta H$, represent the calculated frequencies.

of the lines and asymmetry of the quadrupole triplets (Figs. 8 and 9). Moreover, deviations of the quantization axis from the magnetic field direction have been observed. These studies have shown that allowance for the second-order effects makes it possible to describe all the features of the ENDOR spectra and to obtain accurate values of the hyperfine and quadrupole interaction constants. Sets of these constants for some of the crystals are listed in Table I.

Even a cursory glance at this table reveals delocalization of the wave cloud of an unpaired F-center electron: the values of the electron wave function ($|\psi_0(\mathbf{R}^{(i)})|^2$) obtained from the ENDOR data by means of Eq. (2.2) are large at points fairly distant from a vacancy.

An analysis of the constants of the isotropic hyperfine interaction of an F-center electron with nuclei in the first a^I and second a^{II} spheres in various alkali halide crystals has revealed interesting empirical relationships[12,28]

$$a^I d^3 = \text{const (metal)}, \qquad a^{II} d^5 = \text{const (halogen)}, \tag{5.1}$$

where d is the lattice constant.

Another interesting result of the ENDOR measurements is the nonmonotonic fall of the electron density as the distance r from a defect increases. In the frequently employed effective-mass approximation the smeared-out part of the wave function of a localized electron is usually approximated by the hydrogenic function. Then, $\ln|\psi|^2$ should decrease linearly with increasing r. However, for LiF, NaCl, and some other

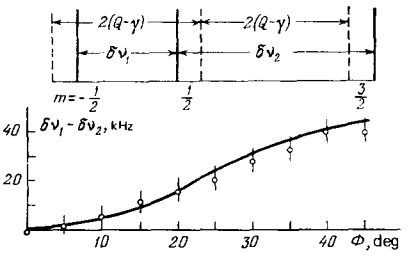

FIG. 9. Asymmetry of the quadrupole triplet of ^{41}K nuclei in sphere I of an F center in KCl (Ref. 17). The circles are the experimental values ($T = 300$°K, $M = -\frac{1}{2}$) and the curve is theoretical.

TABLE I. Hyperfine and Quadrupole Interaction Constants of F Centers in Alkali Halide Crystals (MHz).

Crystal	Sphere	Type of nucleus	a	$b_1=\frac{1}{2}\left(\widetilde{B}_{zz}+\frac{1}{3}(\widetilde{B}_{xx}-\widetilde{B}_{yy})\right)$	$b_2=\frac{1}{3}(\widetilde{B}_{xx}-\widetilde{B}_{yy})$	$Q'=\frac{3}{2}\widetilde{Q}_{zz}$	$Q''=\frac{1}{2}(\widetilde{Q}_{xx}-\widetilde{Q}_{yy})$	$\lvert\psi_0\rvert^2$ at. units
KBr Refs. 12, 90	I	^{39}K	18.228	0.769		0.190		0.0873
	II	^{81}Br	42.740	2.740	0.073	0.220		0.0380
	III	K	0.262	0.022		$\leqslant$0.001		0.0012
	IV	Br	5.716	0.411		0.112		0.00508
	V	K	0.153	0.013	0.0005	±0.003	±0.004	0.000733
	VI	Br	0.820	0.083	0.011	±0.028	±0.010	0.000729
	VIII	Br	0.540	0.064	0.001	±0.009		0.00048
	X	Br	0.158	0.028	0.0008	±0.020		0.00016
KCl Refs. 17, 26	I	^{39}K	20.780	0.924		0.190		0.0995
	II	^{35}Cl	6.908	0.528	0.011	0.033	−0.002	0.0157
	III	K	0.314	0.028		0.005		0.0015
	IV	Cl	1.051	0.106		±0.0017		0.0024
	V	K	0.133	0.018	0.007	±0.010	±0.008	0.00064
	VI	Cl	0.102	0.024	0.0004	±0.0057	±0.005	0.00023
	VIII	Cl	0.081	0.018				0.00018
	IX	K	0.030	0.006				0.00014
NaCl Ref. 19	I	^{23}Na	61.650	3.090				0.0522
	II	^{35}Cl	12.630	1.061	0.007	−0.005	0.005	0.0285
	III	Na	0.334	0.168				0.00028
	IV	Cl	0.466	0.067		±0.0035		0.0011
	V	Na	0.618	0.098				0.00052
	VI	Cl	0.252	0.040	0.003	±0.0032	±0.001	0.00057
	VIII	Cl	0.272	0.033	0.002	±0.0003	±0.0008	0.00062
	IX	Na	0.026	0.035				0.000022
LiF Refs. 13, 27	I	^{7}Li	38.15	3.062				0.0219
	II	^{19}F	105.94	14.96				0.0252
	III	Li	0.497	0.688				0.00028
	IV	F	0.47	1.13				0.00011
	V	Li	0.20	0.333	0.016			0.00012
	VI	F	0.880	0.740	0.050			0.00021
	VIII	F	1.34	0.56	0.02			0.00032
	IX	Li	0.072	0.105				0.000041

crystals the values of $\ln|\psi_0(\mathbf{R}^{(i)})|^2$ not only do not fit a straight line but show even some rise for VI-VIII spheres (Table I). However, it should be noted that other theories of the F-centers[29] also failed to explain all the characteristics of the hyperfine and quadrupole interactions. Some success has been achieved only for the F centers in KCl (Ref. 30).

We shall point out also some useful applications of the ENDOR data. The values of $|\psi|^2$ at the lattice sites can be used to reconstruct approximately the form of the wave function throughout all space[19,31] and the values of $Q_{pq}^{(i)}$ can be used to find the distribution of charges near a paramagnetic center.[32]

b) F_A center. This is one of the centers which appear in alkali halide crystals doped with "foreign" alkali ions. In comparing the ENDOR spectra of the F and F_A centers in KCl:Li (Fig. 10, Ref. 33), we can easily see that the spectrum of the latter centers has strong lines due to Li nuclei; the K nuclei in the first sphere give rise to two sets of lines, α and β, which differ in respect of the hyperfine interaction constants. The change in their hyperfine interaction is due to a redistribution of an electron cloud associated with the appearance of a "foreign" ion. The angular dependences of the Li lines are of the kind shown in Fig. 7; therefore, the Li nucleus should be on a ⟨100⟩ axis. These properties can be explained by just one model of the F_A center: an electron is captured by a halogen vacancy one of the ions in the immediate environment of which is replaced by a "foreign" one. Some redistribution of the wave function of a localized electron[34,35] should have resulted in a monotonic fall away from the ion. The nonmonotonic distortion of the electron cloud observed for the F_A(Li) centers in KCl (Refs. 32 and 35) is probably associated with the noncentral location of the Li ion in KCl (Ref. 36).

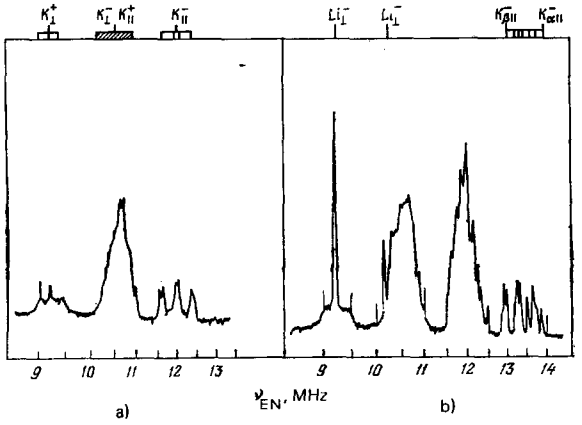

FIG. 10. Part of the ENDOR spectrum of the F centers (a) and F_A centers (b) in KCl:Li, corresponding to nuclei in sphere I (Ref. 33).

c) M and R centers. According to earlier ideas,[37] these are aggregates of F centers: M represents two neighboring F centers (with the symmetry axis along ⟨110⟩) and R consists of three neighboring centers (symmetry axis ⟨111⟩), as shown in Fig. 11. The ENDOR of these centers has not been observed in the ground state. The ESR line of the R centers is masked by the F-center line and the M centers are diamagnetic. However, they can be investigated in a metastable state with a maximum total spin, which is the triplet state of the M centers ($S=1$) and the quartet state of the R centers ($S=3/2$).[38] The results of investigations have confirmed the above models of the centers. In particular, the electron density at the $K_{1\alpha}$ nucleus is approximately equal to the sum of the electron densities created at this point by each F center. The observed difference (10%) is due to the overlap of the wave functions of the F centers.

d) Z centers. These centers form on introduction of divalent impurities (Ca, Sr, Ba, Ir) into alkali halide crystals. The nuclei of the majority of divalent impurities do not have a magnetic moment and, therefore, there are no additional lines in the ENDOR spectra. For this reason it is difficult to determine accurately the location of such impurities. However, the interaction of a paramagnetic-center electron with a divalent ion or with a vacancy compensating the double charge of this ion imposes a characteristic imprint on the hyperfine and quadrupole interaction of this electron with nuclei in the environment of the center. An analysis of these interactions makes it possible to reduce considerably the range of likely models.

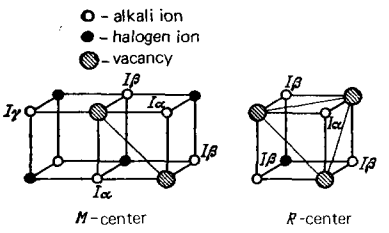

FIG. 11. Aggregate centers in alkali halide crystals.

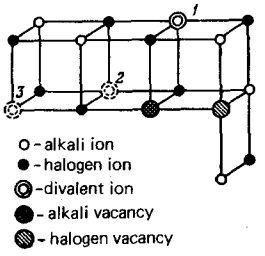

FIG. 12. Models of the Z_1 centers in alkali halide crystals (Ref. 40).

The ENDOR measurements have been carried out only for the Z_1 centers.[39] It has been found that their spectra are in many respects similar to the spectra of the F centers but the nuclei in the immediate environment of a Z_1 center are not equivalent and are characterized by a hyperfine interaction much stronger than that which applies in the case of an F center. The strong perturbation of the electron cloud is due to the influence of the alkali vacancy and not of the divalent ion. This is supported by the slight (1%) difference between the frequencies of the Z_1 centers in crystals containing Ca^{2+} and Sr^{2+} impurities. These properties are exhibited by the model of the Z_1 centers shown in Fig. 12 (Refs. 39 and 40). The existence of these centers is confirmed by the various ENDOR spectra[39] resulting from the fact that the divalent ion can occupy nonequivalent (relative to the F center and positive vacancy) positions.

e) H_2O^- center in KCl (Ref. 41). Photochemical reactions in a KCl:OH crystal may generate an unusual paramagnetic and paraelectric defect, which is an H_2O^- center. Since the optical absorption band of the H_2O^- center has a similar wavelength and width as an F band, it can be regarded as an F center perturbed by the water molecule. Figure 13a shows, for comparison, the well-known spectrum of the F centers in KCl at 78° K. The H_2O^- spectrum at $T > 30$° K (Fig. 13b) has the same nature and angular dependence, indicating its cubic symmetry. At 46.38 MHz there is an additional line which shows no angular dependence and which is the ENDOR line of protons. All the lines of the D_2O^- center (Fig. 13c) are doubly split and the two new positions of the lines differ slightly from the H_2O^- case. This is due to the presence of D_2O^- and HDO^- centers in partly (80%) deuterated crystals and is clear evidence of the presence of two protons in a center. The line splitting is clearly associated with the difference between the amplitudes of the zero-point vibrations of H and D.

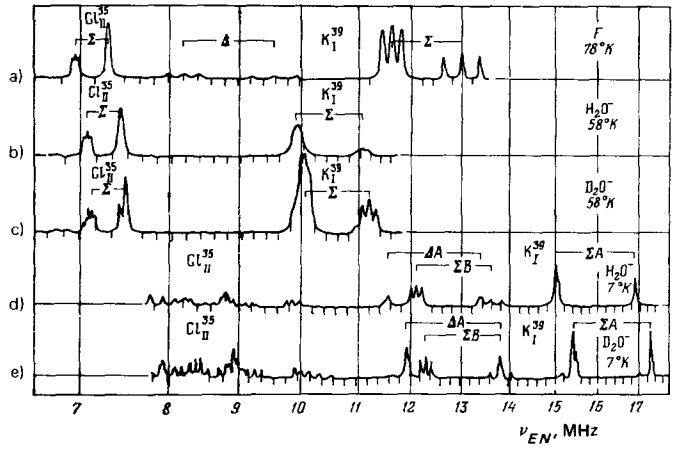

FIG. 13. ENDOR spectra of F, H_2O^-, and D_2O^- centers in KCl (Ref. 41).

When the temperature is varied, the ENDOR spectrum of an H_2O^- center undergoes surprising changes. Cooling of potassium chloride broadens the ENDOR lines which disappear at 30° K. Below 15° K a quite different ENDOR spectrum is observed (Figs. 13d and 13e). The combined $^{39}K_I$ lines split into two well separated groups ΣA and ΣB, indicating that the six nuclei of the nearest neighbors are nonequivalent. The hyperfine interaction with protons at $T < 15$° K becomes anisotropic. Such a change in the ENDOR spectrum as a result of cooling is due to localization of the water molecule impurities at fixed positions. At high temperatures ($T > 30$ °K) the molecule begins to rotate rapidly and this gives rise to the F-like cubic symmetry of the centers.

6. ENDOR OF HOLE CENTERS

Investigations of hole centers in alkali halide and alkaline-earth halide crystals by the ESR method have achieved some success. For example, information has been obtained about the sturcture of the simplest of them, which is a self-localized hole or a V_K center.[42] It has been found that a V_K center has a spin of $\frac{1}{2}$ and exhibits a strongly anisotropic hyperfine interaction with a pair of halogen nuclei.[43] The symmetry axis of the hyperfine interaction is oriented along ⟨110⟩ in alkali halides and along ⟨100⟩ in alkaline-earth halides. This suggests that a hole is localized at two neighboring halogens, i.e., that the V_K center is a negative quasimolecular halogen ion X_2^- (for example, F_2^- in LiF). More complex V_F, V_t, and H centers have also been detected.[44] It has also been found that considerable concentrations of hole centers can be obtained only as a result of doping of alkali and alkaline-earth halides with "foreign" ions. The question is whether an impurity is incorporated in such centers. The ESR investigations have made it possible to study the hyperfine interaction with a pair of nuclei in an X_2^- molecule and the next two nuclei along the axis of the center; this information then leads to the models of the centers shown in Fig. 14. However a full understanding of the structure and properties of hole centers had to wait for ENDOR studies.[20,45-50]

a) V_K center. Investigations of ENDOR spectra have shown that there are no lattice imperfections (compensating vacancies or impurities) in the immediate environment of a self-localized hole. An analysis of the angular dependences of the ENDOR frequencies of all the investigated spheres confirmed the reasonableness of the above model.[42]

The experimental values of the constants of the isotropic and anisotropic hyperfine interaction of a hole with the nuclei in its environment (according to Ref. 20, these are the A, B, C, D, E, and F spheres for a V_K center in LiF and A, B, C, D, F, and G spheres for a V_K center in NaF; the spheres are labeled as shown in

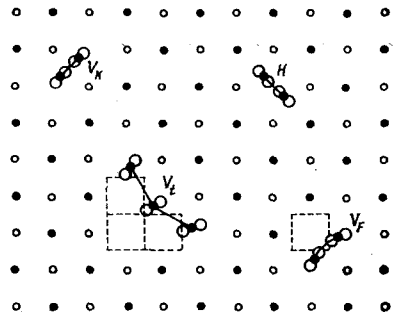

FIG. 14. Hole centers in alkali halide crystals (Ref. 44).

Fig. 15) have revealed a fine effect, which is a static displacement of the ions in the V_K centers.[51] It has been found that localization of a hole in an alkali halide crystal is accompanied by lattice deformation as a result of which the nuclei of a pair of ions which have captured a hole are brought closer together by 0.4 Å, whereas the nuclei in the sphere A move away from the center of the X_2^- molecule.

Had the hyperfine magnetic field at the nuclei been created only by an unpaired σ_u electron of a V_K center, the isotropic hyperfine interaction of the nuclei in the spheres A and B lying in the nodal plane of the molecular orbital of the σ_u electrons would have vanished and the interaction of the nuclei in the other spheres would have been positive. However, the experimental results indicate that the isotropic hyperfine interaction constants of the nuclei in the spheres A, B, C, D, and E are negative. This is evidence of the polarization, by an unpaired σ_u electron, of the molecular oribtals in the inner shells. Under these conditions the magnetic field at the nucleus is the sum of the field of an unpaired electron and an oppositely directed field in the polarized core. The isotropic hyperfine interaction constant can then be negative. A similar polarization of the cores has been recorded for the V_K centers in alkali halide crystals as well as in CaF_2, BaF_2, (Ref. 49), and SrF_2 (Ref. 50).

We shall mention another interesting observation relating to hole centers in alkali and alkaline-earth halides. When an external magnetic field is oriented at right-angles to the axis of the V_K center, lines of forbidden nuclear transitions at frequencies $2\nu_n$, $3\nu_n$, and $4\nu_n$ appear in the ENDOR spectrum.[52] The intensity of these transitions decreases strongly when the field orientation is altered by just 1°. These transitions occur because of the strong anisotropy of the hyperfine interaction of a hole with the nuclei in its environment $A_\parallel/A_\perp \sim 20$ or more). Consequently, when the angle between the axis of a center and the direction of the magnetic field approaches 90°, the gap between the spin levels of

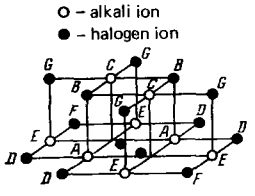

FIG. 15. Model of a V_K center.

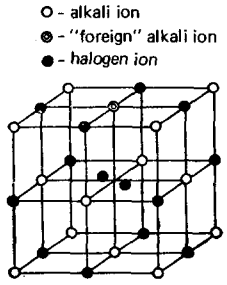

FIG. 16. Model of an H_A center.

a V_K center decreases greatly and a fairly strong indirect interaction between nuclear spins then appears. Consequently, the rf field reorients simultaneously two, three, or even four nuclear spins.

b) *V_{KA} center.* The ESR spectrum of V_{KA} centers, discovered and investigated some time ago,[20,46] resembles the spectrum of the V_K centers. However, ENDOR studies have shown that in the case of V_{KA} center in NaF one of the nearest Na atoms is replaced by Li. The hyperfine interaction characteristics of the V_{KA}(li) centers in NaF are similar to the characteristics of the V_K centers in NaF and LiF. Some differences between the isotropic hyperfine interaction constants may be attributed to the lattice distortion near Li in (Ref. 46).

c) *H center.* Investigations of the optical absorption in ESR of KCl, KBr, and LiF crystals irradiated with x rays revealed[44] a correspondence between the optical H bands and radiation defects, whose symmetry axis was found to be directed along ⟨110⟩ (however, the H band of LiF was not identified). It was suggested that the H centers are intrinsic lattice defects, each of which is an X_2^- molecule replacing a halogen ion (Fig. 14). However, experiments on the ENDOR of these ⟨110⟩ defects in LiF (Ref. 47) have shown that the immediate environment of such a molecule must have a monovalent "foreign" Na impurity ion (Fig. 16). Centers with other positions of the impurity relative to the X_2^- molecule have also been found.[53] Search for a "pure" intrinsic defect in LiF has shown that this is an X_2^- molecule which replaces a halogen ion and is oriented along the ⟨111⟩ axis: the ENDOR method demonstrates that within 11 spheres of the environment there are no other defects.[48]

7. ENDOR OF ELECTRON IMPURITY CENTERS

By way of illustration, we shall concentrate mainly on the impurities investigated in greatest detail by the ENDOR method.

a) *Impurities in silicon.* Chronologically the first experiments by the ENDOR method were carried out on centers formed as a result of doping of silicon with donors belonging to the fifth group (P, As, Sb).[1] They made it possible to determine $|\psi|^2$ at five sites of the silicon lattice. It was found that the wave function of a donor electron does not decrease monotonically on increase of the distance from the donor. This behavior of $|\psi|^2$ can be explained by the complex structure of the conduction band of silicon. It is known that[54]

$$\psi(\mathbf{r}) = \frac{1}{\sqrt{6}} \sum_{j=1}^{6} F_j(\mathbf{r})\, u_j(\mathbf{r})\, e^{i\mathbf{k}_0^j \mathbf{r}}; \qquad (7.1)$$

the index j labels - in the quasimomentum space - various minima $\mathbf{k}_0^j$ of energy in the conduction band, which lie along the ⟨100⟩ axes in silicon; $u_j(\mathbf{r})\exp(i\mathbf{k}_0^j\mathbf{r})$ is the Bloch wave function for the j-th minimum; $F_j(\mathbf{r})$ is the smeared-out wave function. Interference of six terms in Eq. (7.1) is responsible for the nonmonotonic behavior of $|\psi|^2$. The experimental values of $|\psi|^2$ agree to within 50%) with those calculated if the theoretical parameter k_0 is $0.85k_{max}$. In contrast ot the effective masses, the position of the minimum of the bottom of the conduction band k_0 cannot be deduced from cyclotron resonance experiments. Use of ENDOR data makes it possible to determine k_0.

Later and more detailed investigations of the ENDOR of donors belonging to the fifth group[22,55,56] have yielded the hyperfine interaction constants of 20 different coordination spheres (containing about 150 nuclei). Some of the nuclei responsible for specific ENDOR lines are quite easy to identify after analysis of the isotropic and anisotropic hyperfine interactions (these are the [004], [440], [333], and [111] nuclei; see Fig. 17). Other nuclei can be identified on the basis of the ENDOR measurements under uniaxial compression[55] along the ⟨001⟩ direction (⟨115⟩ nuclei). However, this leaves a large group of lines not identified with specific nuclei. The identification process would have been helped by calculations of $|\psi|^2$. However, it is found that the wave function in the effective mass method is only very approximate and, in principle, cannot describe the observed effects. For example, silicon contains [444] and [44$\bar{4}$] nuclei or [224] and [22$\bar{4}$]. The wave function values found by the effective mass method using a Hamiltonian with an inversion symmetry are the same at all these points. Experimental results do not reveal lines of such nuclei (they would have been easy to identify because of twice as high intensity as the intensity, taken as unity, of the ENDOR lines of nuclei of the same class of symmetry but without an inversion partner, for example, [33$\bar{3}$] and [115]). However, pair of lines with a unit intensity but somewhat different (by about 8%) constants of the isotropic hyperfine interaction are observed. Consequently, the values of the correct wave function of an electron at the points [444] and [44$\bar{4}$] should differ. The insufficiency of the wave function of the (7.1) type is also manifested by the fact that for different spheres the best agreement between the theoretical and experimental values of $|\psi|^2$ is obtained for different values of k_0. All this indicates that the effective mass method and its improvec versions[54,58] found seemingly satisfactory for shallow donors should be dropped in the present case. Numerical methods are now being developed for determining the wave function of a donor electron and these are based on the expansion in terms of the Bloch functions of all the points in the Brillouin zone for several energy bands.[57] These methods make it possible, in particular, to identify the nuclei responsible for the majority of the observed ENDOR lines (see Fig. 17) and to find the values of $|\psi|^2$ at these nuclei subject to an rms error of 11% (Ref. 57).

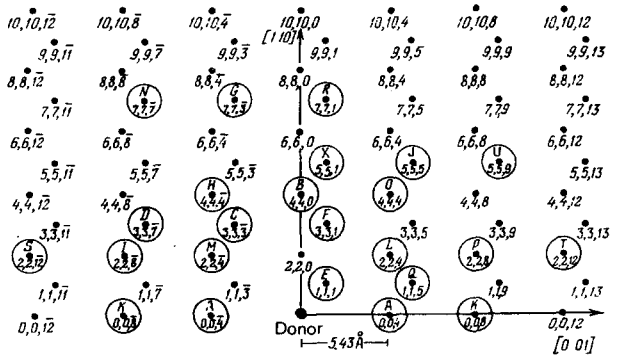

FIG. 17. Schematic diagram showing lattice sites surrounding a donor in silicon. Circles surround sites at which ENDOR lines (identified by capital letters) have been identified.[57]

b) Investigations of ENDOR involving impurity nuclei. An interesting illustration of the high precision of the ENDOR method is the discovery of anomalies of the magnetic hyperfine structure in studies of impurity ions in crystals. Measurements indicate that for some isotopes [^{121}Sb and ^{123}Sb in Si (Ref. 59), ^{6}Li and ^{7}Li in Si (Ref. 1), ^{151}Eu and ^{153}Eu in CaF_2 (Ref. 14), and ^{155}Gd and ^{157}Gd in CeO_2 (Ref. 60)] the ratio of the isotropic hyperfine interaction constants differs by 0.5-1% from the ratio of the nuclear magnetic moments. This difference can be explained by allowing for the following factors: i) the nucleus has a finite volume (which differs for the two isotopes) over which the electron density is spatially distributed; ii) the nuclear magnetic dipole moment is differently distributed in the isotopes; iii) the amplitude of the thermal vibrations near the equilibrium positions is different for the two isotopes and the quantity recorded experimentally is over the vibrations.

c) A very useful and sometimes the only possible means for establishing the model of a center is enrichment of a crystal with isotopes. For some elements (C, O, Ca, Sr, etc.) the natural abundance of the isotopes with nonzero magnetic moments of the nuclei is small. The presence of these elements in a paramagnetic center can be deduced only indirectly. The situation changes if we carry out ENDOR measurements on crystals which are deliberately enriched with isotopes with nonzero nuclear moments. For example, enrichment with the ^{17}O isotope has made it possible to show that in the formation of trigonal centers of Yb^{3+} in CaF_2 the complex $Ca^{2+}F_8^-$ is replaced by $Yb^{3+}F_7^-O^{2-}$, or $Yb^{3+}H^-O_4^{2-}$ (Ref. 61). Measurements of ENDOR in MgO crystals enriched with ^{17}O have been very fruitful.[62]

8. INFLUENCE OF EXTERNAL AGENCIES ON ENDOR SPECTRA

Investigations of the influence of external agencies on ENDOR spectra meet with considerable experimental difficulties. For example, splitting of the ENDOR lines by an electric field is observed—because of the considerable importance of the second-order effects—only in fairly high fields; it is difficult to subject a crystal to a strong but homogeneous deformation (inhomogeneous deformation broadens the ENDOR line), measurements at high temperatures are awkward to carry out, etc. However, the effort put into overcoming these difficulties is repaid by completely new information on the local

field in a crystal, deformation near a defect, spin–phonon interactions, etc.

a) ENDOR in an external electric field. 1) Deĭgen and Roĭtsin[63] noted that electric-field effects may be manifested in ENDOR spectra. They pointed out that all the nuclei in the environment of a paramagnetic center are located at points which are not centrosymmetric even if the paramagnetic center as a whole has an inversion symmetry. Therefore, a spin Hamiltonian describing the ENDOR spectrum contains experssions linear in respect of the electric field and one may expect to observe shifts and splittings of the ENDOR lines.[63,64] The first observations of this effect were made on F centers in alkali halide crystals.[65-67] It was found that the splitting of the ENDOR lines is associated mainly with a change in the isotropic hyperfine interaction constant: the electron cloud is apparently "blown away" from a vacancy by an electric field. The isotropic interaction constant of one of the magnetically equivalent nuclei lying along the axis parallel to the direction of the field and passing through the vacancy increases by an amount $\delta/2 = (da/d\mathbf{E})\cdot\mathbf{E}$ and the constant of the other nucleus decreases by the same amount. The splitting of the ENDOR lines of such a pair of nuclei in the $I^{(1)}=I^{(2)}=\frac{1}{2}$ case (calculations of the frequencies and intensities of ENDOR lines in an electric field for this and more complex cases can be found in Refs. 65 and 68) is

$$\Delta\nu = \sqrt{\delta^2+4\gamma^2}; \qquad (8.1)$$

here, γ is a constant representing a second-order structure (Fig. 8).

Clearly, in weak electric fields ($\delta \leq \gamma$) the splitting is a quadratic function of the field intensity, whereas in strong fields such that $\delta \gg \gamma$, it is proportional to the field. Since $\gamma \propto a^2/4g\beta H$, it is difficult to observe the electric-field effect in those cases when the hyperfine interaction constants are large. It is necessary either to apply very strong electric fields or in some way to reduce the influence of the second-order effects. The latter can be done by increasing the ESR frequency and, consequently, H, by the use of the isotopic replacement of some of the nuclei by others characterized by very different magnetic moments. The first approach has made it possible[67] to observe both linear (in the case of the ^{7}Li nuclei in the first sphere) and quadratic (for the ^{19}F nuclei in the second sphere) electric-field dependences for the F centers in LiF. Enrichment of $^7Li^{19}F$ with the ^{6}Li isotope has made it possible to observe the electric field effects in nuclei in the first sphere in much weaker fields.[66]

The results of experiments on the ENDOR of F centers in an electric field[65-67] are collected in the column headed "Experiment" in Table II. Apart from the F centers in alkali halides, the splitting of ENDOR lines in an electric field has been observed also for F_A(Li) centers in KCl and KBr (Ref. 69), for AsO_4^{4-} in KH_2AsO_4 (Ref. 70), and for radiation defects in triglycine sulfate.[71]

2) A microtheory of electric-field effects in ENDOR spectra must provide means for calculating constants of the $da/d\mathbf{E}$ type as a function of the characteristics of paramagnetic centers and of the crystal which contains them.[67,72,73] The smallness of the electric-field constants means that one can use perturbation theory in calculating them.

We can show that[74]

$$\delta a^{(i)} \approx -\frac{2ea^{(i)}}{\bar{\Delta}} \int_0^{R^{(i)}} (d\mathbf{r},\ \mathbf{E}+\eta(\mathbf{r})\mathbf{E}+\lambda(\mathbf{r})\mathbf{E}); \qquad (8.2)$$

here, $\bar{\Delta}$ is the average distance between the ground and excited states; $\mathbf{E}+\eta(\mathbf{r})\mathbf{E}+\lambda(\mathbf{r})\mathbf{E}$ is the local electric field acting on an electron. This field comprises the macroscopic field $\mathbf{E}$, the field of induced dipoles $\eta(\mathbf{r})\mathbf{E}$ in an ideal crystal, and distrotions of the electric field by a defect $\lambda(\mathbf{r})\mathbf{E}$. In the case of F centers the investigated nuclei are at the lattice sites and the integral of the periodic function $\eta(\mathbf{r})$ vanishes. If we simulate approximately the vacancy-induced distortion of the electric field by the field of a point dipole,[67] we find that the right-hand side of Eq. (8.2) has no free parameters. The values of $|da/dE|$ calculated by means of Eq. (8.2) are listed in the column headed "Theory" in Table II.

The agreement between the theory and experiment for an F center in an alkali halide crystal leads us to hope that even in more complex cases the expression (8.2) can be used to determine the unknown characteristics of the local electric field or of a paramagnetic center. For example, the electric field near an F_A(Li) center in an

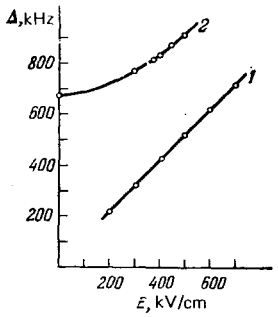

FIG. 18. Dependences of the splitting of ENDOR lines of F centers in LiF on the applied electric field directed along the "vacancy–investigated nucleus" axis:[67] 1) ^{7}Li in sphere I, $\mathbf{E}\|\mathbf{H}$; 2) ^{19}F in sphere II, $\mathbf{E}\perp\mathbf{H}$. The curves are theoretical dependences plotted in accordance with Eq. (8.1).

TABLE II. Electrohyperfine Constants of F Centers in Alkali Halide Crystals.

Crystal	Sphere	Nucleus	$\lvert da/dE\rvert$, Hz · cm · V^{-1}	
			Experiment	Theory
KBr	I	^{39}K	1.00±0.05	0.85
	II	^{81}Br	2.00±0.05	2.00
	IV	^{81}Br	0.33±0.02	0.38
KCl	I	^{39}K	0.9±0.05	0.83
	II	^{35}Cl	0.25±0.03	0.28
	IV	^{35}Cl	0.05±0.005	0.06
NaCl	I	^{23}Na	2.00±0.5	2.0
	II	^{35}Cl	0.5±0.05	0.375
LiF	I	^{6}Li	0.36±0.03	0.26
	I	^{7}Li	0.96±0.01	0.675
	II	^{19}F	1.21±0.02	1.21

alkali halide crystal is distorted not only by the presence of a vacancy but also by the difference between the displacements of the Li ion and the host ions in the electric field. If we ignore this difference, the calculated value of $da^{(Li)}/dE$ is half that observed. It is possible to match the theoretical and experimental results by selecting the following differences between the displacements: $u^{Li}-u^{Cl}=3.1(u^{K}-u^{Cl})$ in the case of KCl:Li, but $u^{Li}-u^{Br}=2.55(U^{K}-u^{Br})$ for KBr:Li (Ref. 69).

b) ENDOR in the presence of external stresses. The application of external uniaxial or hydrostatic compressive stresses produces displacements of the lattice ions and such displacements alter the distribution of the electron density of a paramagnetic center. This changes the hyperfine and quadrupole interaction constants and gives rise to the experimentally observed shifts and splittings of the ENDOR frequencies.[55,75-81] Typical changes in the ENDOR spectra are shown in Fig. 19.

1) We shall first consider the description of an ENDOR spectrum in the presence of stresses. An analysis of the ENDOR spectra of crystals deformed by external stresses can be divided arbitrarily into three stages. In the first stage the analysis is based on some form of description of the ion displacements (strain tensor, symmetrized linear combinations of the displacements of the nuclei) and group-theoretic methods are used to obtain phenomenological spin Hamiltonians which allow for the deformation of a crystal.[77,82-84] The changes in the hyperfine and quadrupole interaction constants can then be expressed in terms of the characteristics of the ion displacements, for example, in terms of the components of the tensor of the elastic constants $s_{\alpha\beta\gamma\delta}$. In the case of the hyperfine interaction of nuclei of the [00n] type in a cubic crystal subjected to, for example, uniform compression by a pressure p along the k axis, we obtain[82]

$$\delta a=-p\,[a_1(s_{11}+2s_{12})+a_3(s_{11}-s_{12})(3k_z^2-1)]+\ldots; \qquad (8.3)$$

a_1 and a_3 are phenomenological parameters representing the change in the hyperfine interaction due to the applied pressure (they are known as the piezohyperfine constants). The shifts of the ENDOR lines of shallow donors in silicon (Fig. 19), observed on compression along the ⟨001⟩ axis, could be described more conveniently not by Eq. (8.3) but by expressions of the type[55]

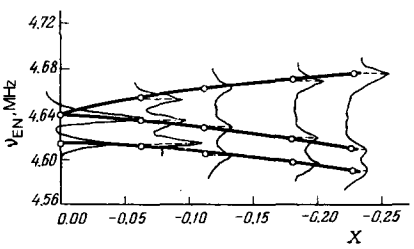

FIG. 19. Dependences of the shift and splitting of the ENDOR lines in sphere $B[4,4,0]$ of Sb in silicon on the pressure applied along the ⟨001⟩ axis.[55] $\mathbf{H}\|\langle 100\rangle$. The lines of the nuclei along the y and z axes become split, and those along the x and y axes shift in parallel.

$$\Delta a_\alpha=-e_\alpha X-f_\alpha X^2, \qquad X=\frac{\Theta_u s}{6\Delta}; \qquad (8.4)$$

e_α and f_α are the piezohyperfine constants; Θ_u is the deformation potential constant; Δ is the valley–orbit splitting; s is proportional to the pressure (the coefficient of proportionality is a combination of the elastic constants). A description of the measured shifts and splitting of ENDOR lines by means of expressions such as Eqs. (8.3)-(8.4) makes it possible to separate effects which are linear and nonlinear in respect of the strain and to find the phenomenological constants.

In the second stage a method similar to that described in subsection 2a above gives explicit expressions for the piezohyperfine constants.[82] It is then possible to use the ENDOR data to determine the characteristics of deformation of a crystal near a defect. For example, it has been established that the substitution of macroscopic values of $s_{\alpha\beta\gamma\delta}$ in Eq. (8.3) ensures agreement between the calculated and observed line shifts only for nuclei far from a defect. In the case of nuclei close to a defect the theory and experiment differ by an amount considerably greater than the error in the calculation of the piezohyperfine constants. This suggests that the deformation near a defect is inhomogeneous and that the elastic constants are now different from the elastic constants of the original crystal. In this way it is found that near an F center in an alkali halide crystal the elastic constants differ by a factor of 2-5 from the bulk values.[77,85] It has also been established that the local compressibility of CaF_2 near an interstitial gadolinium ion is only 0.7 of the compressibility of the host crystal.[79]

There are still unsolved problems which may give information on even finer local properties of crystals. For example, in the case of the F centers in alkali halide crystals neither the homogeneous deformation approximation, used to derive Eq. (8.3), nor the replacement of the elastic constants in Eq. (8.3) by the local values is capable of explaining the observed dependence of the shift of the ENDOR lines of the nuclei in the first sphere on the orientation of the uniaxial compression axis k in a plane perpendicular to the line toward the nucleus, i.e., on k_x and k_y.

Finally, in the third stage the dependence of the ion displacements near a defect on external stresses is calculated. This is a problem in the microtheory of elasticity; the results obtained in the preceding stage can be used here to check the validity of the calculation methods. In particular, it has been found for CaF_2:Gd that the microtheory of elasticity[86] predicts a local compressibility which is in agreement with the results of the ENDOR experiments.[79]

2) The calibration of pressures is a technically difficult task at low temperatures and a method for performing this task is suggested in Ref. 79. It is pointed out there that in the case of CaF_2:Gd the anisotropic hyperfine interaction of gadolinium with nuclei in the second sphere is described sufficiently precisely if it is assumed that the electron and nuclear spins interact as if they were point dipoles. Since the dipole–dipole interaction is inversely proportional to the cube of the distance between the dipoles, the change in the anisotropic

hyperfine interaction on the application of pressure—recorded by the ENDOR method—can be used to find the pressure. Cyrstals of this kind can then be used as standards in pressure measurements.

3) Piezohyperfine interaction and spin–lattice relaxation will now be discussed. Many spin–lattice relaxation processes are due to the modulation of the hyperfine interaction by the thermal lattice vibrations and are governed by the values of the coefficients in the expansion of the hyperfine interaction in terms of the nuclear displacements. These coefficients are independent of the cause of the displacement (thermal vibrations or external stresses) and are the piezohyperfine interaction constants. For example, if the hyperfine interaction with nuclei in the first sphere surrounding a paramagnetic center is predominant, only a_1 and a_3 determine the transition probability in a direct relaxation process. Determination of these coefficients by the ENDOR method makes it possible to calculate the relaxation times using familiar formulas. In this way it is possible to suggest a method for determination of the spin–lattice relaxation constants from ENDOR data. The relaxation time of F centers in KCl calculated by this method[82] is 72 min, which is in agreement with the directly measured[87] value of 83 min.

c) Influence of temperature on ENDOR spectra. Investigations of the temperature dependence of the hyperfine and quadrupole interaction constants can give information on the spin–phonon interaction, on the nature of ion vibrations near a defect, and on the relative positions of the electron energy levels of a paramagnetic center.[12,13,88-93] Naturally, a suitable level of theory is required for this purpose.

A change in the termperature of a crystal redistributes the populations of the electron levels of paramagnetic centers and of the phonon levels of the host crystal. In the case of paramagnetic centers for which the average gap between the ground and excited states $\bar{\Delta}$ is comparable with k_BT, we must allow for redistributions of the populations of the electron and phonon levels, whereas in the case of paramagnetic centers with $\bar{\Delta} \gg k_BT$ we can confine ourselves to allowance for the redistribution of the phonon level populations. The usual phenomenological description of the temperature dependences observed under a constant pressure is as follows. Let G be one of the spin Hamiltonian constants. Then,[94]

$$\left(\frac{dG}{dT}\right)_p = \left(\frac{dG}{dV}\right)_T \left(\frac{dV}{dT}\right)_p + \left(\frac{dG}{dT}\right)_V. \qquad (8.5)$$

The first term describes the implicit temperature dependence of G associated with the thermal expansion of the crystal. The thermal expansion coefficient $(dV/dT)_p$ is usually known and the value of $(dG/dV)_T$ is either regarded as a parameter or is estimated using, for example, the empirical rules of Eq. (5.1). The second term represents the direct influence of the lattice vibrations on the constant G. It is convenient to represent it in the form $(dG/dT)_V T = G^{(2)}\langle u\rangle^2$, where $\langle u\rangle^2$ is the square of the ion displacement amplitude averaged over all the lattice vibrations and $G^{(2)}$ is a phenomenological parameter. If the vibration spectrum of a crystal is known, we can find the temperature dependence of $\langle u\rangle^2$. It is usual to approximate the real temperature dependence by the expression $\langle u^2\rangle = C\cdot\coth(\theta/T)$. Comparing the experimental temperature dependence with theory, we can then find the spin–phonon interaction constant $G^{(2)}$, the characteristic temperature of the crystal Θ, and other parameters. In this way the spin–phonon constants of the F electrons have been determined from the changes, in the 4.2-570°K range, in the hyperfine and quadrupole interactions in spheres I-VIII of the F centers in alkali halide crystals.[89,90] It is interesting to note that the changes in some of the constants (a^{IV} for LiF, Q^{IV} for NaCl, etc.) can be of the same order of magnitude as the constants themselves.

If the temperature dependence of the hyperfine interaction constants is governed by local vibrations of ions near a defect, it becomes possible to find the frequencies of local vibrations.[92]

The capabilities of the ENDOR method in comparative estimates of the amplitudes of vibrations of various ions near a defect are demonstrated in Ref. 93. A comparison of the temperature dependences of the isotropic hyperfine interaction with the Li nuclei in the F_A(Li) centers and with the K nuclei in the F centers in KCl and KBr (Fig. 20) suggests that the amplitude of the Li ion vibrations is several times greater than that of the K ions.

One must mention the interesting experiments carried out on interstitial Li donors in silicon.[91] The lowest state of this system has fivefold orbital degeneracy (doublet E and triplet T_2) because of the special nature of the valley–orbit splitting. In the absence of deformation, the electron relaxation times are fairly short and ENDOR is not observed. Application of a uniaxial pressure along [001] lifts the degeneracy, increases the relaxation times, and creates favorable conditions for observing the ENDOR spectra. The constant of the isotropic hyperfine interaction with the Li nuclei determined by the ENDOR method is found to increase by a factor of 10

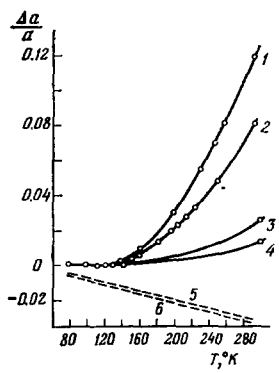

FIG. 20. Temperature dependences of the relative changes in the isotropic hyperfine interaction constants of the F and F_A(Li) centers in KCl (1,3, and 5) and in KBr (2,4, and 6). The points are the experimental results and the continuous curves are theoretical; the dashed line represents the calculated contribution of the thermal expansion of the host crystals (5,6). 1), 2) ^{7}Li, F_A(Li) centers;[93] 3), 4) ^{39}K, sphere I of F centers.[89,90]

when the temperature is raised from 1.3 to 4 °K. This is explained by the thermal population of the E and T_2 orbital states and averaging of the hyperfine interaction over these states. A comparison of the experimental results with the microtheory makes it possible to determine the hyperfine interaction for each of the states and to find the energy gap between the states.

9. ENDOR DYNAMICS

The term ENDOR dynamics is taken to refer to the study of the dependence of the ENDOR signal on the amplitudes of the microwave and the rf alternating fields H_1 and H_2, on the detuning of the magnetic field $H - H_0$ (H_0 corresponds to the center of the ESR line), and on the frequencies and intensities of additional radiation interacting with the nuclear system.[1,12,95-102]

a) Positive ENDOR. An increase in microwave absorption due to passage through a nuclear resonance (see Sec. 2), known as positive ENDOR, can be described as follows. The intensity of an inhomogeneously broadened hyperfine ESR line is given by[103]

$$W = \frac{\pi}{2}\chi_0 H_1 \int_0^\infty \frac{\nu' \tilde{g}(\nu - \nu')\, h(\nu' - \nu_0)\, d\nu'}{1 + \frac{\pi}{4} g^2\beta^2 H_1^2 T_1 \tilde{g}(\nu - \nu')}, \qquad (9.1)$$

where $\nu_0 = g\beta H_0$; χ_0 is the static spin susceptibility; $\tilde{g}(\nu - \nu')$ is the function describing the profile of a spin packet; $h(\nu' - \nu_0)$ is the packet distribution function; T_1 is the spin–lattice relaxation time. Additional radiation at the frequency of the nuclear transition ν_n gives rise to a new relaxation channel (Fig. 2). The time $T_1^* = \alpha T_1$ representing relaxation under these conditions depends in the usual way on ν_n and on the amplitude of the rf field H_2 ($\alpha \leq 1$ is the degree of reduction in the relaxation time T_1 by the rf field). The change in the ESR signal, i.e., the steady-state ENDOR effect, is

$$\delta W = W^* - W; \qquad (9.2)$$

here, W^* is the intensity of the ESR line in the presence of rf radiation. The function $\tilde{g}(\nu - \nu')$ is usually approximated by a Lorentzian of width $\Delta\nu_L = T_2^{-1}$ (T_2 is the spin–spin relaxation time) and the function $h(\nu' - \nu_0)$ is replaced by a Gaussian of specific width $\Delta\nu_f$. The ENDOR results allow us to identify the interaction of a paramagnetic center with just the resonating (f-th) nuclei. The sources of local broadening fields are the nuclei whose constants are smaller than those of the f-th nuclei. Each sphere has its own value of $\Delta\nu_f$, so that the experimental results give a family of curves representing saturation of the ENDOR signal by a microwave field (Fig. 21). A comparison of the ENDOR signal intensities obtained for different values of H, H_1, H_2, and ν_n with expressions such as (9.1) and (9.2) allows us to determine the relaxation times T_1, T_2, and T_1^*. These relaxation times are not only physically valuable, because they give information on the spin–lattice and spin–spin relaxation mechanisms, but they are also of practical importance because they can be used to guide an investigator in the selection of the optimal conditions for recording the ENDOR signal.

The theory of the steady-state ENDOR effect has been improved by allowing for the influence of the cross-relaxation processes and heating of the dipole reservoir of electron spins.[96,97] The corss-relaxation effects have been observed experimentally.[97]

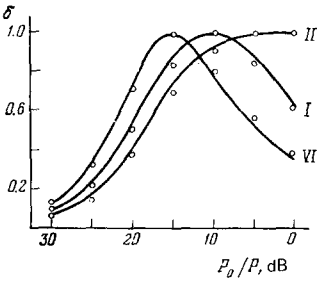

FIG. 21. Curves showing saturation of ENDOR signals by a microwave field in KBr (Ref. 97). $T = 77$°K, $\mathbf{H} \| \langle 100 \rangle$. The axes give the attenuation of the microwave field power ($P_0 = 18$ mW) and the relative intensity of the signal. The curves are theoretical and the points are the experimental values. The three curves are plotted for spheres I, II, and VI.

b) Negative ENDOR.[98] In some cases an increase in the rf field intensity H_2 up to 5-10 Oe reduces the microwave absorption, i.e., a negative ENDOR effect is observed. The mechanism of this effect is not quite clear. The characteristics of the negative effect - a high (compared with the positive resonance) signal intensity of some of the nuclei and a weak dependence on the relaxation processes - suggest possible applications.

c) Distant ENDOR, i.e., ENDOR due to distant nuclei.[99] If the nuclear spins are coupled weakly to the lattice, the only effective nuclear relaxation process is the diffusion of the excitation along a crystal followed by the transfer of energy via paramagnetic centers to the lattice. Under these conditions the absorption of rf power by nuclei distant from the paramagnetic centers alters the ESR signal giving rise to distant ENDOR. This distant effect is characterized by the absence of a shift of the resonance frequency (the distant nuclei interact weakly with the paramagnetic centers); the time for the recovery of the ESR signal after the rf field is switched off is governed by the nuclear spin–lattice relaxation processes, whereas in the convetnional ENDOR mechanism the recovery time is of the order of the electron spin–lattice relaxation time.

d) ENDOR of homogeneous ESR lines.[100] A necessary condition for the observation of the conventional ENDOR signal (Sec. 2) is the saturation of an inhomogeneously broadened ESR line. For some systems, for example, in the case of collodial particles of lithium in LiF, the ESR lines are homogeneous and their positions are governed by the sum of an external magnetic field and the field created by the polarized (by lowering the temperature of the crystal or by the Overhauser effect[5]) nuclei. The depolarization of the nuclei by the rf field displaces the ESR line as a whole. The change in the ESR at a fixed value of an external field is then recorded as the ENDOR signal.

e) ENDOR due to "forbidden" transitions.[101] The intensity of the conventional ENDOR signal due to allowed

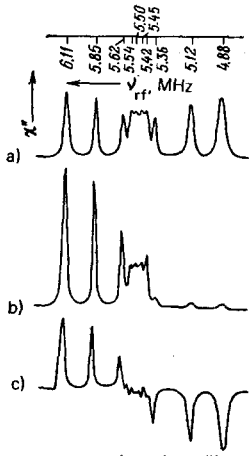

FIG. 22. Spectra of nuclei in spheres III and V of an F center in LiF recorded in different ways:[102] a) without additional rf field (conventional ENDOR); b) with additional rf field for the difference line in sphere IV; c) triple electron–nuclear–nuclear resonance.

ESR transitions is approximately given by $\delta W \approx W\tau_1/\tau_x$. This intensity is low if $\tau_x \gg \tau_1$. In the case of coupled electron–nuclear systems, for example, when $A_{\parallel} \approx \nu_n$, one may encounter forbidden ESR transitions characterized by $\Delta M = \pm 1$ and $\Delta m \neq 0$ (Ref. 5). When these transitions are saturated, the intensity of the ENDOR signal is $\delta\tilde{W} \approx \tilde{W}\tau_x/\tau_1$. Although $W \gg W$, we can also have cases when $\delta\tilde{W} \gg \delta W$. Then, intense ENDOR signals due to forbidden transitions should occur in the samples characterized by $\tau_x \gg \tau_1$.

f) ENDOR with two rf fields. The use of an additional rf field in the steady-state ENDOR gives rise to new relaxation channels. For example, if the field corresponds to the gap between the levels $|-\frac{1}{2}0\rangle$ and $|-\frac{1}{2}1\rangle$ (Fig. 2), the following relaxation process becomes effective:

$$\left|\tfrac{1}{2}1\right\rangle \xleftrightarrow{P_n} \left|\tfrac{1}{2}0\right\rangle \xleftrightarrow{\tau_1} \left|-\tfrac{1}{2}0\right\rangle \xleftrightarrow{P_n'} \left|-\tfrac{1}{2}1\right\rangle.$$

Then certain lines are amplified selectively (by an order of magnitude or more), as shown in Fig. 22, the ENDOR spectrum becomes simpler,[102] and its interpretation is easier.

If the frequency of the main rf field is fixed at the frequency of the ENDOR line of one of the nuclei and the frequency of the additional rf field is varied, it is possible to record the signals due to other nuclei as a change in the intensity of this line (this is known as the triple electron–nuclear–nuclear resonance - Fig. 22). It is interesting to note that the lines in the spectrum associated with different projections of the electron spin are recorded on opposite sides of the zero line; the indeterminacy in the attribution of a transition to the sum or difference frequencies then disappears. This circumstance is useful in the determination of the relative signs of the spin-Hamiltonian constants.

We shall conclude by noting that investigations of ENDOR dynamics not only give information on the mechanisms of the relaxation of nuclei near a defect, but provide one of the ways of tackling certain practical tasks, such as the polarization of nuclear spins in crystals.

10. OPTICAL DETECTION OF ENDOR

Recording any number of optical quanta (photons) is easier than recording the same number of microwave quanta. Therefore, optical methods for detecting ESR and ENDOR signals are several orders of magnitude more sensitive than the usual observation methods. In the optical detection of transitions between the nuclear sublevels one can use any method for the optical recording of the ESR signal.[104]

We shall describe the idea behind one of these methods, which has been used successfully in studies of F centers in alkali halide crystals.[105,106] This method utilizes the signal of magnetic circular dichroism, which is the difference between the absorption of right- and left-handed circularly polarized light, traveling along the direction of an applied magnetic field. Optical transitions occur between the magnetic-field-split levels of the ground-state doublet and a P band of excited states. The dichroism signal is a function of the difference between the populations of the doublet sublevels. The change in the populations, due to the microwave resonance field, alters the dichroism signal, providing an optical indication of the ESR of the ground state of the F centers. The whole optical pumping cycle which occurs in the observation of the magnetic circular dichroism of the F centers includes the absorption of a polarized photon and excitation to the absorption band, nonradiative decay to a relaxed excited state, luminescence from this state to an unrelaxed ground state, and nonradiative decay to the normal (relaxed) ground state. Since the spin projection is conserved in the luminescence from the relaxed excited state and in the nonradiative transition to the normal ground state, spin transitions to the relaxed excited state redistribute the populations of the ground-state sublevels. The changes in the dichroism signal which accompany such transitions represent the ESR signal of the relaxed excited state.

The changes in the ESR of the ground or excited states of an F center recorded by the dichroism method on application of an rf field (optical triple resonance) can be used to study the hyperfine and quadrupole interactions of the ground and relaxed excited states. One should only bear in mind that the short lifefime τ of a given center in the relaxed excited state imposes restrictions on the resolution of the method ($\Delta\nu \sim 1/\pi\tau$) and requires high rf fields H_2 [the ENDOR signal is maximal if $(g_n\beta_n H_2\tau)^2 \geq 1$].

The methods for optical detection of the ESR and ENDOR signals give important information on the nature of the excited state. In particular, in the case of the F centers in KI it was found that the spectra of the relaxed excited states are not affected by rotation of the crystal in a magnetic field, which is evidence of the isotropy of the g factor and of the hyperfine interaction of such states.[106] This behavior can be explained by assuming that the dynamic Jahn–Teller effect occurs in the relaxed excited states.[107] In this case the averaging over the vibronic coordinates has the result that the electron density contains only the sums of the squares of three orbitals and does not exhibit an angular dependence. In the

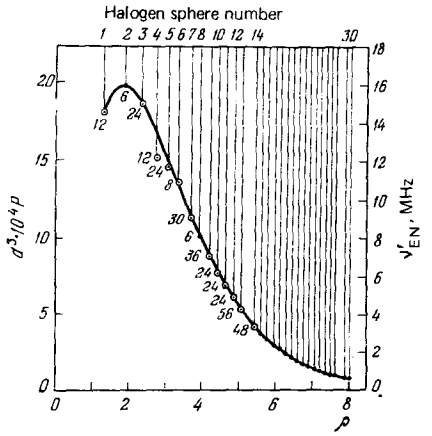

FIG. 23. Dependence of the electron density in a relaxed excited state on the distance for F centers in KI (Ref. 106); $\nu'_{EN} = \nu_{EN} - \nu_n$, $d = 3.525$ Å. The circles are the experimental results and the numbers represent the number of nuclei in a sphere. The curve corresponds to Eq. (10.1) with $\eta = 0.515$.

range of distances ($r > d$) corresponding to the relaxed excited states the potential acting on an electron can be regarded as being of the Coulomb type and the experimentally determined electron density can be approximated by functions of the type

$$P = \frac{\eta^3}{3\pi}(\eta\rho)^2 e^{-2\eta\rho}, \qquad \rho = \frac{r}{d}, \tag{10.1}$$

when η is a free parameter. The good agreement between experiment and theory (Fig. 23) is evidence of the reasonableness of this assumption.

11. USE OF THE ENDOR METHOD IN DETERMINATION OF FUNDAMENTAL CHARACTERISTICS OF CRYSTALS

The varied information obtained by the ENDOR method can be used to determine not only the properties of paramagnetic centers but also the fundamental characteristics of crystals containing them. We shall now consider some such applications.

a) Band structure of crystals. We mentioned earlier that the first step in this direction was made by Feher.[1] He compared the measured values of the hyperfine interaction constants of shallow donors in silicon with the theoretical values of $|\psi|^2$ and found the position of the minimum of the bottom of the conduction band $\mathbf{k}_0$ in k space. A method for the determination of the structure of the conduction band of crystals on the basis of the ENDOR data is given in Ref. 108. The idea of the method is as follows. Let $\psi_0(\mathbf{R}_p)$ be the value of the wave function of a paramagnetic center deduced from the measured isotropic hyperfine interaction constant $a^{(p)}$. We then apply the effective mass method to find the wave function ψ of an electron for a number of variants of the band structure (spherical constant-energy surface, ellipsoidal constant-energy surfaces, etc.). This function contains, as the parameters of the band structure, the components of the effective mass tensor μ_i ($i = 1, 2, 3$) and the position of the minimum of the bottom of the conduction band in k space k_0^j (j is the number of the valley). Comparing the theoretical $\psi(\mathbf{R}_p, \mu_i, k_0^j \ldots)$ and experimental $\psi_0(\mathbf{R}_p)$ values, we can determine not only μ_i and k_0^j but also the actual band structure variant appropriate to a given crystal.

This method was applied to the energy band structures of LiF, NaF, NaCl, KCl, and KBr crystals.[109] Although the theoretical wave functions were fairly rough, the effective masses found in this way were of the same order of magnitude as those measured by the cyclotron resonance method. Further progress would require improvements in the theory of local centers. The advantages of this method lie in the direct determination of the effective masses of the band electrons and not of polarons (in contrast to the studies based on cyclotron resonance and transport phenomena) and also in the fact that the method is free of the requirements of a sufficiently high current carrier density, long mean free time, etc.

b) Local electric field in ENDOR.[74] It is shown in Sec. 8 that the splitting of ENDOR lines in an external electric field is goverened by the local field. When the vector drawn from a paramagnetic center to a given nucleus is an integral multiple of the lattice vector, the integral in Eq. (8.2) containing the characteristics of the local field $\eta(\mathbf{r})$ vanishes. However, in other cases [if for reasons of symmetry the term $\eta(\mathbf{r})$ does not drop out on the right-hand side of Eq. (8.2)], the ENDOR line splittings can be used to find the integrated characteristics of the local field.

c) Deformation potential. A comparison of the ENDOR line shifts caused by uniaxial compression with Eq. (8.4) makes it possible to find X and, consequently, the deformation potential constant Θ_u. In carrying this out it is assumed that the values of s and Δ are deduced from independent experiments, while e_α and f_α are obtained from microtheory. The values of Θ_u obtained in this way[55] are in agreement with those deduced by other methods.

12. CONCLUSIONS

Our examples illustrate the potentialities of the ENDOR method in investigations of the interaction of electron and nuclear spins and of the reactions of these spins to external agencies, as well as in investigations of the structure and properties of impurity centers in crystals, spin–phonon interactions, and fundamental characteris tics of the host crystal itself. The application of the ENDOR method to studies of the hyperfine structure of the ESR spectrum, which is masked by the inhomogeneous line broadening, is particularly effective. In order to determine a structure, it is sometimes convenient to use the discrete saturation method.[110] However, if the hyperfine structure is due to interaction with a large number of different nuclei and whenever constants have to be determined with a high precision, the ENDOR method becomes irreplaceable.

The achievements of the ENDOR method have stimulated research on a variety of other combined resonances. They include double resonances in which one or both electromagnetic fields are replaced by acoustic vibrations at the resonance frequency (double acousto-magnetic electron–nuclear resonance,[111] double magneto-acoustic

electron–nuclear resonance[112]). The idea of recording weak transitions at another higher frequency underlies the optical methods for the detection of magnetic resonances, double magnon–nuclear resonance,[113] and many other double resonances.[114]

The accumulated experience in applying the ENDOR method clearly shows it to be exceptionally fruitful and promising. The authors hope that the present review will stimulate further ENDOR investigations.

[1]G. Feher, Phys. Rev. **114**, 500, 834 (1956); **114**, 1219, (1959); G. Feher and E. A. Gere, Phys. Rev. **114**, 1245 (1959).
[2]H. Seidel and H. C. Wolf, Phys. Status Solidi **11**, 3 (1965).
[3]H. Seidel and H. C. Wolf, in: Physics of Color Centers (ed. by W. B. Fowler), Academic Press, New York, 1968, Chap. 8.
[4]S. Geschwind, in: Hyperfine Interactions in Solids (Russ. Transl., Mir, M., 1970), p. 103.
[5]A. Abragam and B. Bleaney, Electron Paramagnetic Resonance of Transition Ions, Oxford University Press, 1970 (Russ. Transl., Vol. 1, Mir, M., 1972; Vol. 2, Mir, M., 1973).
[6]A. L. Kwiram, Annu. Rev. Phys. Chem. **22**, 133 (1971).
[7]J. M. Baker, E. R. Davies, and T. R. Reddy, Contemp. Phys. **13**, 45 (1972).
[8]C. P. Slichter, Principles of Magnetic Resonance with Examples from Solid State Physics, Harper and Row, New York, 1963 (Russ. Transl., Mir, M., 1967).
[9]C. P. Poole, Experimental Techniques in Electron Spin Resonance, Wiley, New York, 1966 (Russ. Transl., Mir, M., 1970).
[10]M. A. Ruban, Avtorskoe svidetel'stvo SSSR (Author's Certificate), No. 219 862, appl. January 23, 1965, publ. June 14, 1968.
[11]G. Feher, Bell Syst. Tech. J. **36**, 449 (1957).
[12]H. Seidel, Z. Phys. **165**, 218, 239 (1961); Z. Angew. Phys. **14**, 21 (1962).
[13]W. C. Holton and H. Blum, Phys. Rev. **125**, 89 (1962).
[14]J. M. Baker and F. I. B. Williams, Proc. R. Soc. London Ser. A **267**, 283 (1962); M. F. Deĭgen, M. A. Ruban, and Yu. S. Gromovoĭ, Fiz. Tverd. Tela (Leningrad) **8**, 826 (1966) [Sov. Phys. Solid State **8**, 662 (1966)]; D. Schmid, Phys. Status Solidi **18**, 653 (1966); R. J. Cook, J. Sci. Instrum. **43**, 548 (1966); N. Boden, J. Capart, W. Derbyshire, H. S. Gutowsky, and J. R. Hansen, Rev. Sci. Instrum. **39**, 805 (1968); T. G. Castner and A. M. Doyle, Rev. Sci. Instrum. **39**, 1090 (1968); E. R. Davies and J. P. Hurrell, J. Phys. E **1**, 847 (1968); Yu. F. Mitrofanov and Yu. E. Pol'skiĭ, Tr. Kazakh. Aviats. Inst. **129**, 46 (1970); A. Fourrier-Lamer and T. Lenoir, C. R. Acad. Sci. Ser. B **272**, 98 (1971); J. Hrycej, Czech. J. Phys. A **22**, 346 (1972); D. Schmalbein, A. Witte, R. Roder, and G. Laukien, Rev. Sci. Instrum. **43**, 1664 (1972); W. T. Doyle, T. F. Dutton, and A. B. Wolbarst, Rev. Sci. Instrum. **43**, 1668 (1972); N. Arakawa, Kotai Butsuri **7**, 107 (1972); T. C. Christidis and F. W. Heineken, J. Phys. E **6**, 432 (1973); E. R. Davies, Phys. Lett. A **47**, 1 (1974); S. S. Ishchenko and S. M. Okulov, Prib. Tekh. Eksp. No. 5, 144 (1975); K. Gruber, J. Forrer, A. Schweiger, and H. H. Gunthard, J. Phys. E **7**, 569 (1974).
[15]D. Halford, Phys. Rev. **127**, 1940 (1962); J. H. N. Loubser and A. C. J. Wright, Diamond. Res. 16 (1973).
[16]T. E. Feuchtwang, Phys. Rev. **126**, 1628 (1962); L. C. Kravitz and W. W. Piper, Phys. Rev. **146**, 322 (1966).
[17]S. S. Ishchenko. Avtoreferat kand. dissertatsii (Author's Abstract of Thesis for Candidate's Degree), Institute of Semiconductors, Academy of Sciences of the Ukrainian SSR, Kiev, 1970.
[18]J. M. Baker and J. P. Hurrell, Proc. Phys. Soc. London **82**, 742 (1963); M. M. Zaripov and L. Ya. Shekun, Paramagnitnyĭ rezonans (Paramagnetic Resonance), Kazan University, 1964; M. F. Deĭgen, M. A. Ruban, S. S. Ishchenko, and N. B. Barin, Zh. Eksp. Teor. Fiz. **51**, 1014 (1966) [Sov. Phys. JETP **24**, 676 (1967)]; H. A. Buckmaster, R. Chatterjee, and Y. H. Shing, Phys. Status Solidi A **13**, 9 (1972); J. S. M. Harvey and H. Kiefte, J. Phys. B **3**, 1326 (1970).
[19]M. F. Deĭgen, Vis. Akad. Nauk Ukr. RSR No. 6, 18 (1969).
[20]R. Gazzinelli and R. L. Mieher, Phys. Rev. **175**, 395 (1968); D. F. Daly and R. L. Mieher, Phys. Rev. **175**, 412 (1968); I. L. Bass and R. L. Mieher, Phys. Rev. **175**, 421 (1968).
[21]Yu. G. Semenov, Ukr. Fiz. Zh. **19**, 1467 (1974).
[22]E. B. Hale and R. L. Mieher, Phys. Rev. **184**, 739 (1969).
[23]A. B. Wolbarst, Phys. Status Solidi B **49**, 571 (1972).
[24]M. M. Zaripov, V. K. Kaĭbiyaĭnen, V. P. Meĭklyar, and M. L. Falin, Fiz. Tverd. Tela (Leningrad) **17**, 1229 (1975) [Sov. Phys. Solid State **17**, 798 (1975)].
[25]R. J. Cook and D. H. Whiffen, Proc. Phys. Soc. London **84**, 845 (1964); J. Chem. Phys. **43**, 2908 (1965); J. M. Baker and W. B. J. Blake, Phys. Lett. A **31**, 61 (1970); J. Phys. C **6**, 3501 (1973); J. A. R. Coope, N. S. Dalal, C. A. McDowell, and R. Srinivasan, Mol. Phys. **24**, 403 (1972); W. Kolbe and N. Edelstein, Phys. Rev. B **4**, 2859 (1971); Yu. F. Mitrofanov, Yu. E. Pol'skiĭ, and M. L. Falin, Zh. Eksp. Teor. Fiz. **61**, 1486 (1971) [Sov. Phys. JETP **34**, 790 (1972)].
[26]R. Kersten, Phys. Status Solidi **29**, 575 (1968).
[27]N. P. Baran, Avtoreferat kand. dissertatsii (Author's Abstract of Thesis for Candidate's Degree), Institute of Semiconductors, Academy of Sciences of the Ukrainian SSR, Kiev, 1969.
[28]C. E. Bailey, Ph.D. Thesis, Dartmouth College, Hanover, N. H., 1968.
[29]B. S. Gourary and F. J. Adrian, Phys. Rev. **105**, 1180 (1957); Solid State Phys. **10**, 127 (1960); J. K. Kübler and R. J. Friauf, Phys. Rev. **140**, A1742 (1965); J. E. Lowther, Physica (Utrecht) B+C **79**, 148 (1975); J. Schmid. Phys. Kondens. Mater. **15**, 119 (1972).
[30]R. F. Wood, Phys. Status Solidi **42**, 849 (1970).
[31]A. Gold, J. Chem. Phys. **35**, 2180 (1961).
[32]R. Kersten, Solid State Commun. **8**, 167 (1970).
[33]R. L. Mieher, Phys. Rev. Lett. **8**, 362 (1962).
[34]N. P. Baran, M. F. Deĭgen, S. S. Ishchenko, M. A. Ruban, and V. V. Udod, Fiz. Tverd. Tela (Leningrad) **10**, 3005 (1968) [Sov. Phys. Solid State **10**, 2370 (1969)]; H. Ohkura, K. Miyoshi, and Y. Mori, J. Phys. Soc. Jpn. **27**, 790 (1969).
[35]Yu. V. Fedotov, N. P. Baran, and S. S. Ishchenko, Fiz. Tverd. Tela (Leningrad) **16**, 341 (1974) [Sov. Phys. Solid State **16**, 225 (1974)].
[36]F. Rosenberger and F. Luty, Solid State Commun. **7**, 983 (1969); M. F. Deigen, V. S. Viknin, and M. D. Glinchuk, Phys. Status Solidi B **53**, 391 (1972).
[37]C. Z. van Doorn and Y. Haven, Philips Res. Rep. **11**, 479 (1956); C. Z. van Doorn, Philips Res. Rep. **12**, 309 (1957); H. Pick, Z. Phys. **159**, 69 (1960).
[38]H. Seidel, Phys. Lett. **7**, 27 (1963); H. Seidel, M. Schwoerer, and D. Schmid, Z. Phys. **182**, 398 (1964); Yu. V. Fedotov, N. N. Bagmut, and I. V. Matyash, Fiz. Tverd. Tela (Leningrad) **14**, 612 (1972) [Sov. Phys. Solid State **14**, 519 (1972)].
[39]J. C. Bushnell, Thesis, University of Illinois, Urbana-Champaign, Ill., 1964.
[40]F. Rosenberger and F. Luty, Solid State Commun. **7**, 249 (1969).
[41]W. Rusch and H. Seidel, Phys. Status Solidi B **63**, 183 (1974).
[42]W. Kanzig, Phys. Rev. **99**, 1890 (1955).
[43]T. G. Castner and W. Kanzig, J. Phys. Chem. Solids **3**, 178 (1957); T. O. Woodruff and W. Kanzig, J. Phys. Chem. Solids **5**, 268 (1958); W. Hayes and J. W. Twidell, Proc. Phys. Soc. London **79**, 1295 (1962).
[44]W. Kanzig and T. O. Woodruff, J. Phys. Chem. Solids **9**, 70 (1959); W. Kanzig, J. Phys. Chem. Solids **17**, 80, 88 (1960).
[45]R. Gazzinelli and R. L. Mieher, Phys. Rev. Lett. **12**, 644

(1964).
[46]I. L. Bass and R. L. Mieher, Phys. Rev. Lett. **15**, 25 (1965).
[47]M. L. Dakss and R. L. Mieher, Phys. Rev. **187**, 1053 (1969); Phys. Rev. Lett. **18**, 1056 (1967).
[48]Y. H. Chu and R. L. Mieher, Phys. Rev. **188**, 1311 (1969).
[49]R. F. Marzke and R. L. Mieher, Phys. Rev. **182**, 453 (1969).
[50]R. Gazzinelli, G. M. Ribeiro, and M. L. de Siqueira, Solid State Commun. **13**, 1131 (1973).
[51]D. F. Daly and R. L. Mieher, Phys. Rev. Lett. **19**, 637 (1967); Phys. Rev. **183**, 368 (1969).
[52]Yu. S. Gromovoĭ, V. G. Grachev, M. F. Deĭgen, and V. V. Teslenko, Fiz. Tverd. Tela (Leningrad) **16**, 2639 (1974) [Sov. Phys. Solid State **16**, 1712 (1975)].
[53]W. J. Plant and R. L. Mieher, Phys. Rev. B **7**, 4793 (1973).
[54]W. Kohn and J. M. Luttinger, Phys. Rev. **97**, 1721 (1955); **98**, 915 (1955).
[55]E. B. Hale and T. G. Castner Jr., Phys. Rev. B **1**, 4763 (1970).
[56]E. B. Hale and R. L. Mieher, Phys. Rev. B **3**, 1955 (1971).
[57]J. L. Ivey and R. L. Mieher, Phys. Rev. Lett. **29**, 176 (1972); Phys. Rev. B **11**, 822, 849 (1975).
[58]R. A. Faulkner, Phys. Rev. **184**, 713 (1969); T. G. Castner Jr., Phys. Rev. B **2**, 4911 (1970); T. H. Ning and C. T. Sah, Phys. Rev. B **4**, 3468 (1971); S. T. Pantelides and C. T. Sah, Solid State Commun. **11**, 1713 (1972); Phys. Rev. B **10**, 621, 638 (1974).
[59]J. Eisinger and G. Feher, Phys. Rev. **109**, 1172 (1958).
[60]J. M. Baker, G. M. Copland, and B. M. Wanklyn, J. Phys. C **2**, 862 (1969).
[61]T. R. Reddy, E. R. Davies, J. M. Baker, D. N. Chambers, R. S. Newman, and B. Ozbay, Phys. Lett. A **36**, 231 (1971).
[62]P. Freund, B. F. Hann, and J. Owen, J. Phys. C **4**, L296 (1971); P. Freund, J. Owen, and B. F. Hann, J. Phys. C **6**, L139 (1973); A. L. Allsop, J. Owen, and A. E. Hughes, J. Phys. C **6**, L337 (1973); P. Freund, J. Phys. C **7**, L33 (1974).
[63]M. F. Deĭgen and A. B. Roĭtsin, Zh. Eksp. Teor. Fiz. **47**, 294 (1964) [Sov. Phys. JETP **20**, 196 (1965)].
[64]A. B. Roĭtsin, Ukr. Fiz. Zh. **10**, 147 (1965); N. I. Deryugina and A. B. Roĭtsin, Ukr. Fiz. Zh. **11**, 594 (1966); N. I. Deryugina, Ukr. Fiz. Zh. **12**, 1892 (1967).
[65]J. F. Reichert and P. S. Pershan, Phys. Rev. Lett. **15**, 780 (1965); Z. Usmani and J. F. Reichert, Phys. Rev. **180**, 482 (1969).
[66]Z. Usmani and J. F. Reichert, Phys. Rev. Lett **24**, 709 (1970).
[67]N. P. Baran, V. G. Grachev, M. F. Deĭgen, S. S. Ishchenko, and L. I. Chernenko, Fiz. Tverd. Tela (Leningrad) **15**, 519 (1973) [Sov. Phys. Solid State **15**, 360 (1973)].
[68]V. G. Grachev, Ukr. Fiz. Zh. **18**, 1669 (1973).
[69]Yu. V. Fedotov, V. G. Grachev, and N. N. Bagmut, Fiz. Tverd. Tala (Leningrad) **15**, 3128 (1973) [Sov. Phys. Solid State **15**, 2094 (1974)]; V. G. Grachev and Yu. V. Fedotov, Fiz. Tverd. Tela (Leningrad) **16**, 2648 (1974) [Sov. Phys. Solid State **16**, 1717 (1975)].
[70]N. S. Dalal, C. A. McDowell, and R. Srinivasan, Phys. Rev. Lett. **25**, 823 (1970).
[71]W. Windsch, M. Welter, and W. Driesel, in: Abstracts of Third Intern. Meeting on Ferroelectricity, Edinburgh, 1973, in: Ferroelectrics **8**, 551 (1974).
[72]M. F. Deĭgen and A. B. Roĭtsin, Zh. Eksp. Teor. Fiz. **59**, 209 (1970) [Sov. Phys. JETP **32**, 115 (1971)].
[73]Z. Usmani and J. F. Reichert, Phys. Rev. B **1**, 2078 (1970).
[74]V. G. Grachev, M. F. Deĭgen, and S. I. Pekar, Fiz. Tverd. Tela (Leningrad) **15**, 2155 (1973) [Sov. Phys. Solid State **15**, 1431 (1974)].
[75]Z. Sroubek, E. Simanek, and R. Orbach, Phys. Rev. Lett. **20**, 391 (1968).
[76]C. E. Bailey, C. I. Burch, W. T. Doyle, and H. P. Liu, in: Proc. Intern. Symposium on Color Centers in Alkali Halides, Rome, 1968, p. 15. H. P. Liu, Thesis, Dartmouth College, Hanover, N.H.
[77]C. E. Bailey, J. Phys. Chem. Solids **31**, 2229 (1970).
[78]A. B. Wolbarst, J. Phys. Chem. Solids **33**, 2013 (1972); Phys. Status Solidi B **51**, 321 (1972).
[79]S. V. Kasatochkin and E. N. Yakovlev, Fiz. Tverd. Tela (Leningrad) **17**, 520 (1975) [Sov. Phys. Solid State **17**, 324 (1975)].
[80]P. H. Zimmermann and R. Valentin, Phys. Rev. B **12**, 3519 (1975).
[81]K. Mamola and R. Wu, J. Phys. Chem. Solids **36**, 1323 (1975).
[82]B. A. Novominskii, Avtoreferat kand. dissertatsii (Author's Abstract of Thesis for Candidate's Degree), Polytechnic Institute, Kiev, 1974.
[83]S. A. Al'tshuler and B. M. Kozyrev, Élektronnyĭ paramagnitnyĭ rezonans soedineniĭ élementov promezhutochnykh grupp (Electron Paramagnetic Resonance of Compounds of Elements in Intermediate Groups), Nauka, M., 1972.
[84]V. G. Grachev and B. A. Novominskii, Fiz. Tverd. Tela (Leningrad) **15**, 2980 (1973) [Sov. Phys. Solid State **15**, 1987 (1974)].
[85]A. B. Wolbarst, Phys. Status Solidi B **55**, 299 (1973).
[86]B. Z. Malkin, Fiz. Tverd. Tela (Leningrad) **11**, 1208 (1969) [Sov. Phys. Solid State **11**, 981 (1969)]; Z. I. Ivanenko and B. Z. Malkin, Fiz. Tverd. Tela (Leningrad) **11**, 1859 (1969) [Sov. Phys. Solid State **11**, 1498 (1970)].
[87]D. W. Feldman, R. W. Warren, and J. G. Castle Jr., Phys. Rev. **135**, A470 (1964); R. W. Warren, D. W. Feldman, and J. G. Castle Jr., Phys. Rev. **136**, A1347 (1964).
[88]V. L. Vinetskiĭ and V. Ya. Kravchenko, Zh. Eksp. Teor. Fiz. **47**, 902 (1964) [Sov. Phys. JETP **20**, 604 (1965)]; V. Ya. Kravchenko and V. L. Vinetskiĭ, Opt. Spektrosk. **18**, 73 (1965) [Opt. Spectrosc. (USSR) **18**, 37 (1965)]; W. T. Doyle, C. Burch, and H. Jones, Bull. Am. Phys. Soc. **12**, 58 (1967); N. P. Baran, M. F. Deĭgen, S. S. Ishchenko, M. A. Ruban, and V. V. Udod, Fiz. Tverd. Tela (Leningrad) **10**, 1250 (1968) [Sov. Phys. Solid State **10**, 996 (1968)].
[89]N. P. Baran, V. G. Grachev, M. F. Deĭgen, and S. S. Ishchenko, Zh. Eksp. Teor. Fiz. **55**, 2069 (1968) [Sov. Phys. JETP **28**, 1094 (1969)].
[90]S. S. Ishchenko, N. P. Baran, M. F. Deĭgen, M. A. Ruban, V. V. Teslenko, and V. V. Udod, Zh. Eksp. Teor. Fiz. **57**, 763 (1969) [Sov. Phys. JETP **30**, 418 (1970)].
[91]G. D. Watkins and F. S. Ham, Phys. Rev. B **1**, 4071 (1970).
[92]W. T. Doyle and A. B. Wolbarst, J. Phys. Chem. Solids **36**, 549 (1975).
[93]Yu. V. Fedotov, V. G. Grachev, and V. K. Bezobchuk, Fiz. Tverd. Tela (Leningrad) **18**, 264 (1976) [Sov. Phys. Solid State **18**, 154 (1976)].
[94]W. M. Walsh Jr., J. Jeener, and N. Bloembergen, Phys. Rev. **139**, A1338 (1965).
[95]T. G. Izyumova and G. V. Skrotskiĭ, Zh. Eksp. Teor. Fiz. **40**, 133 (1961) [Sov. Phys. JETP **13**, 93 (1961)]; G. V. Skrotskiĭ and T. G. Izyumova, Usp. Fiz. Nauk **73**, 423 (1961) [Sov. Phys. Usp. **4**, 177 (1961)]; S. P. Dovgopol and T. G. Izyumova, Zh. Eksp. Teor. Fiz. **49**, 1483 (1965) [Sov. Phys. JETP **22**, 1018 (1966)]; E. C. McIrvine, J. Lambe, and N. Laurance, Phys. Rev. **136**, A467 (1964); J. P. Hurrell, Proc. R. Soc. London Ser. A **283**, 448 (1964); W. T. Doyle and T. F. Dutton, Phys. Rev. **180**, 424 (1969); J. H. Freed, J. Chem. Phys. **43**, 2312 (1965); **50**, 2271 (1969); E. R. Davies and T. R. Reddy, Phys. Lett. A **31**, 398 (1970); N. S. Dalal and C. A. McDowell, Chem. Phys. Lett. **6**, 617 (1970); J. H. Freed, D. S. Leniart, and H. D. Connor, J. Chem. Phys. **58**, 3089 (1973); W. Th. Wenckebach, T. J. B. Swanenburg, and N. J. Poulis, Phys. Rep. (Phys. Lett. C) **14**, 181 (1974); A. V. Duglav, Yu. F. Mitrofanov, and Yu. E. Pol'skiĭ, Fiz. Tverd. Tela (Leningrad) **16**, 186 (1974) [Sov. Phys. Solid State **16**, 111 (1974)].
[96]B. D. Shanina, Avtoreferat kand. dissertatsii (Author's Abstract of Thesis for Candidate's Degree), Institute of Semiconductors, Academy of Sciences of the Ukrainian SSR, Kiev, 1968; V. L. Gokhman and V. D. Shanina, Ukr. Fiz. Zh. **19**, 437 (1974); Fiz. Tverd. Tela (Leningrad) **17**, 1408 (1975) [Sov. Phys. Solid State **17**, 905 (1975)].
[97]A. B. Brik, N. P. Baran, S. S. Ishchenko, and L. A. Shul'man,

Fiz. Tverd. Tela (Leningrad) **15**, 1830 (1973) [Sov. Phys. Solid State **15**, 1220 (1973)]; Zh. Eksp. Teor. Fiz. **67**, 186 (1974) [Sov. Phys. JETP **40**, 94 (1975)]. A. B. Brik and S. S. Ishchenko, Fiz. Tverd. Tela (Leningrad) **18**, 2442 (1976) [Sov. Phys. Solid State **18**, 1425 (1976)].

[98]N. M. Atherton, A. J. Blackhurst, and I. P. Cook, Chem. Phys. Lett. **8**, 187 (1971); I. Miyagawa, R. B. Davidson, H. A. Helms, Jr., and B. A. Wilkinson Jr., J. Magn. Res. **10**, 156 (1973); H. A. Helms Jr., I. Suzuki, and I. Miyagawa, J. Chem. Phys. **59**, 5055 (1973); I. Suzuki, J. Phys. Soc. Jpn. **37**, 1379 (1974); V. L. Gokhman and B. D. Shanina, Fiz. Tverd. Tela (Leningrad) **18**, 946 (1976) [Sov. Phys. Solid State **18**, 542 (1976)].

[99]J. Lambe, N.Laurance, E. C. McIrvine, and R. W. Terhune, Phys. Rev. **122**, 1161 (1961); O. S. Leifson and C. D. Jeffries, Phys. Rev. **122**, 1781 (1961); G. Theobald, C. R. Acad. Sci. Ser. B **268**, 635 (1969); W. T. Wenckebach, L. A. H. Schreurs, H. Hoogstraate, T. J. B. Swanenburg, and N. J. Poulis, Physica (Utrecht **52**, 455 (1971); L. L. Buishvili, M. D. Zviadadze, and N. P. Fokina, Zh. Eksp. Teor. Fiz. **65**, 2272 (1973) [Sov. Phys. JETP **38**, 1135 (1974)]; A. B. Brik, I. V. Matyash, and Yu. V. Fedotov, Zh. Eksp. Teor. Fiz. **71**, 665 (1976) [Sov. Phys. JETP **44**, 349 (1976)].

[100]G. Feher and R. A. Isaacson, J. Magn. Reson. **7**, 111 (1972).

[101]A. B. Brik, I. V. Matyash, and Yu. V. Fedotov, Fiz. Tverd. Tela (Leningrad) **19**, 71 (1977) [Sov. Phys. Solid State **19**, 40 (1977)].

[102]N. P. Baran, A. B. Brik, and S. S. Ishchenko, Zh. Eksp. Teor. Fiz. **64**, 703 (1973) [Sov. Phys. JETP **37**, 357 (1973)].

[103]A. M. Portis, Phys. Rev. **91**, 1071 (1953).

[104]L. N. Novikov, V. G. Pokazan'ev, and G. V. Skrotskiĭ, Usp. Fiz. Nauk **101**, 273 (1970) [Sov. Phys. Usp. **13**, 384 (1970)]; A. L. Kwiram, in: Magnetic Resonance (ed. by C. A. McDowell), University Park Press, Baltimore (1972), p. 271; P. Ehret, G. Jesse, and H. C. Wolf, Z. Naturforsch. Teil A **23**, 195 (1968); P. D. Parry, T. R. Carver, S. O. Sari, and S. E. Schnatterly, Phys. Rev. Lett. **22**, 326 (1969); P. A. Schnegg, C. Jaccard, and M. Aegerter, Phys. Lett. A **42**, 369 (1973); H. Ohkura, K. Murakami, K. Iwamori, S. Nakamura, and Y. Mori, J. Phys. Soc. Jpn. **34**, 275 (1973).

[105]L. F. Mollenauer, S. Pan, and S. Yngvesson, Phys. Rev. Lett. **23**, 683 (1969); L. F. Mollenauer, S. Pan, and A. Winnacker, Phys. Rev. Lett. **26**, 1643 (1971); A. Winnacker and L. F. Mollenauer, Phys. Rev. B **6**, 787 (1972); L. F. Mollenauer and S. Pan, Phys. Rev. B **6**, 772 (1972).

[106]L. F. Mollenauer and G. Baldacchini, Phys. Rev. Lett. **29**, 465 (1972).

[107]F. S. Ham, Phys. Rev. Lett. **28**, 1048 (1972).

[108]V. G. Grachev, M. F. Deĭgen, and S. I. Pekar, Fiz. Tverd. Tela (Leningrad) **9**, 3157 (1967) [Sov. Phys. Solid State **9**, 2489 (1968)]; Proc. Ninth Intern. Conf. on Physics of Semiconductors, Moscow, 1968, Vol. 2, publ. by Nauka, Leningrad (1968), p. 1130.

[109]W. B. Fowler and A. B. Kunz, Phys. Status Solidi **40**, 249 (1970); V.G. Grachev, M.F. Deigen, H. I. Neymark, and S. I. Pekar, Phys. Status Solidi B **43**, K93 (1971).

[110]G. Feher and E. A. Gere, Phys. Rev. **114**, 1245 (1959); V. D. Korepanov, A. I. Chernitsyn, and R. A. Dautov, Zh. Eksp. Teor. Fiz. **45**, 385 (1963) [Sov. Phys. JETP **18**, 266 (1964)]. P. I. Bekauri, B. G. Berulava, T. I. Sanadze, and O. G. Khakhanashvili, Zh. Eksp. Teor. Fiz. **52**, 447 (1967) [Sov. Phys. JETP **25**, 292 (1967)]. P. I. Bekauri, B. G. Berulava, T.I. Sanadze, O. G. Khakhanashvili, and G. R. Khutsishvili, Zh. Eksp. Teor. Fiz. **59**, 368 (1970) [Sov. Phys. JETP **32**, 200 (1971)]; T. A. Abromovskaya, B. G. Berulava, and T. I. Sanadze, Zh. Eksp. Teor. Fiz. **66**, 306 (1974) [Sov. Phys. JETP **39**, 145 (1974)].

[111]C.M. Bowden, H. C. Meyer, and P. F. McDonald, Phys. Lett. **22**, 224 (1969); H. C. Meyer, C. M. Bowden, and P. F. McDonald, Rev. Sci. Instrum. **40**, 730 (1969).

[112]M. F. Deĭgen and I. I. Zheru, Fiz. Tverd. Tela (Leningrad) **9**, 1679, 2611 (1967) [Sov. Phys. Solid State **9**, 1320 (1967); **9**, 2053 (1968)]; V. A. Golenishchev-Kutuzov, U. Kh. Kopvillem, and N. A. Shamukov, Pis'ma Zh. Eksp. Teor. Fiz. **10**, 240 (1969) [JETP Lett. **10**, 151 (1969)]; R. V. Saburova, V. A. Golenishchev-Kutuzov, and N. A. Shamukov, Zh. Eksp. Teor. Fiz. **59**, 1460 (1970) [Sov. Phys. JETP **32**, 797 (1971)].

[113]M. P. Petrov, G. A. Smolenskiĭ, V. F. Panin, and A. P. Paugurt, Usp. Fiz. Nauk **114**, 157 (1974) [Sov. Fiz. Usp. **17**, 798 (1975)].

[114]A.I. Ekimov and V. I. Safarov, Pis'ma Zh. Eksp. Teor. Fiz. **15**, 453 (1972) [JETP Lett. **15**, 319 (1972)]; L. R. Dalton, Magn. Reson. Rev. **1**, 301 (1972); V. A. Golenishchev-Kutuzov, R. V. Saburova, and N. A. Shumakov, Usp. Fiz. Nauk **119**, 201 (1976) [Sov. Phys. Usp. **19**, 449 (1976)].

Translated by A. Tybulewicz